MS No.: acp-2021-860 **MS type:** Measurement report
Title: Measurement Report: Interpretation of Wide Range Particulate Matter Size Distributions in Delhi
Author(s): Ülkü Alver Şahin et al.

RESPONSE TO REVIEWERS (2)

REPORT #1

I appreciate the edits made by the authors throughout the manuscript based on initial set of reviews.

However, I find the response of the authors to not change their current colorscale (jet/rainbow) unsatisfactory.

Authors: "We have used colours commonly found in journal papers, and would prefer not to redraw."

I understand that the aerosol community has used the jet/rainbow colorscale for decades and it is inconvenient for us to change from the "standard" rainbow/jet colorscale. But, given the guidelines, I have to point this out. The Copernicus guidelines (https://www.atmospheric-chemistry-and-physics.net/submission.html#figurestables) clearly state: "For more information on the background and importance of addressing this issue, we refer to Stoelzle & Stein (2021) (https://hess.copernicus.org/articles/25/4549/2021/)." The cited article literally discusses why "rainbow colormap" (color scheme in question) is misleading.

As such, I reiterate, the authors should change the colorscales in figures 4 and 11, S5, S8, and S13 to a uniform colorscale (https://www.nature.com/articles/s41467-020-19160-7)

While it is ultimately the editor's call, I want to note that I have made this comment on other manuscripts — and want to be consistent — where the authors changed to a non-misleading (uniform) colorscale.

RESPONSE: The authors have amended the colorscale in the figures identified by the reviewer in the way requested.

.

Measurement Report: Interpretation of Wide Range Particulate Matter Size Distributions in Delhi

Ülkü Alver Şahin[1], Roy M Harrison[2,a], Mohammed S. Alam[2,b] David C.S. Beddows[2,3], Dimitrios Bousiotis[2], Zongbo Shi[2] Leigh R. Crilley[4], William Bloss[2], James Brean[2], Isha Khanna[5,c] and Rulan Verma[6,c]

[1] Istanbul University-Cerrahpaşa, Engineering Faculty, Environmental Engineering Department, Istanbul, Türkiye

[2] School of Geography, Earth and Environmental Sciences University of Birmingham, Birmingham, B15 2TT, UK

[3] National Centre for Atmospheric Science University of York, Heslington, York, YO10 5DQ, UK

[4] Department of Chemistry, York University Toronto, Ontario, M3J 1P3, Canada

[5] Puget Sound Clean Air Agency, Seattle, Washington, USA 98101

[6] Institute of research on catalysis and the environment of Lyon - IRCELYON Université De Lyon, 69626 Villeurbanne cedex, France

Corresponding author: E-mail: r.m.harrison@bham.ac.uk (Roy M. Harrison)

[a] Also at: Department of Environmental Sciences / Centre of Excellence in Environmental Studies, King Abdulaziz University, PO Box 80203, Jeddah, 21589, Saudi Arabia

[b] Now at: School of Biosciences, University of Nottingham, Sutton Bonington Campus, Leicestershire, LE12 5RD

[c] Previously at: IIT Delhi, Hauz Khas, New Delhi, India 110016

ABSTRACT

Delhi is one of the world's most polluted cities, with very high concentrations of airborne particulate matter. However, little is known on the factors controlling the characteristics of wide range particle number size distributions. Here, new measurements are reported from three field campaigns conducted in winter, pre-monsoon and post-monsoon seasons on the Indian Insitute of Technology campus in the south of the city. Particle number size distributions were measured simultaneously using a Scanning Mobility Particle Sizer and a Grimm optical particle monitor, covering 15 nm to >10 µm diameter. The merged, wide-range size distributions were categorised into five size ranges: nucleation (15-20 nm), Aitken (20-100 nm), accumulation (100 nm-1 µm), large fine (1-2.5 µm) and coarse (2.5-10 µm) particles. The ultrafine fraction (15-100 nm) accounts for about 52 % of all particles by number (PN_{10}-total particle number from 15 nm to 10 µm), but just 1 % by PM_{10} volume (PV_{10}- total particle volume from 15 nm to 10 µm). The measured size distributions are markedly coarser than most from other parts of the world, but are consistent with earlier cascade impactor data from Delhi. Our results suggest substantial aerosol processing by coagulation, condensation and water uptake in the heavily polluted atmosphere, which takes place mostly at nighttime and in the morning hours. Total number concentrations are highest in winter, but the mode of the distribution is largest in the post-monsoon (autumn) season. The accumulation mode particles dominate the particle volume in autumn and winter, while the coarse mode dominates in summer. Polar plots show a huge variation between both size fractions in the same season and between seasons for the same size fraction. The diurnal pattern of particle numbers is strongly reflective of a road traffic influence upon concentrations, especially in autumn and winter, although other sources such as cooking and domestic heating may influence the evening peak. There is a clear influence of diesel traffic at nighttime when it is permitted to enter the city, and also indications in the size distribution data of a mode <15 nm, probably attributable to CNG/LPG vehicles. New particle formation appears to be infrequent, and in this dataset is limited to one day

in the summer campaign. Our results reveal that the very high emissions of airborne particles in Delhi, particularly from traffic, determine the variation of particle number size distributions.

1. INTRODUCTION

Air pollution in Delhi has been studied for many years, and the authorities have implemented several interventions designed to limit the concentrations. The sulphur content of diesel and petrol fuels was reduced to 50 ppm during 1996-2010, more than 1300 industries were shut down due to hazardous emissions, commercial vehicles older than 15 years were gradually taken out of the traffic fleet, and public transport vehicles and auto-ricksaws were converted to compressed natural gas (CNG) fuel (Narain and Krupnick, 2007). An odd–even vehicle number plate restriction has been applied during working days (Chowdhury et al., 2017). Although these measures have reduced gaseous pollutants (SO_2 and CO) and primary particulate matter, in recent years, several studies have reported that the $PM_{2.5}$ concentrations have been constant or slowly increasing in India, especially in the winter and autumn seasons (Babu et al., 2013; Balakrishnan et al., 2019; Dandona et al. 2017, Kumar et al., 2017), except in 2020. In 2020, the $PM_{2.5}$ level decreased by approximately 40 %, due to Covid-19 measures (Rodríguez-Urrego and Rodríguez-Urrego 2020; Mahato et al., 2020). Although the overall emission sources in India are dominated by traffic, industry, construction, and local biomass burning, haze pollution events in Delhi are frequently related to the large-scale open burning of post-harvest crop residues/wood during the crop burning season in nearby rural regions (Cusworth et al. 2018; Bikkina et al. 2019; Kanawade et al., 2020). Furthermore, the sources of particles are mostly local (Hama et al., 2020), meteorological factors play an important role in influencing concentrations of air pollution (Tiwari et al., 2014; Yadav et al., 2016; Guo et al., 2017; Dumka et al. 2019; Kumar et al. 2020).

Annual average $PM_{2.5}$ levels range between 81 and 190 $\mu g/m^3$ in Delhi and are clearly higher than the WHO guideline value (5 $\mu g/m^3$) and Indian national limit value (40 $\mu g/m^3$) (Hama et al., 2020). To the best of our knowledge, most studies in India have focussed on the source apportionment from chemical profiles of particles (Pant and Harrison, 2012; Jain et al. 2020; Bhandari et al., 2020; Rai et al., 2020). Mostly they have reported that biomass burning contributes greatly to $PM_{2.5}$ mass while

traffic contributes heavily to PM_{10} mass in Delhi. Residential energy use contributes 50 % of the $PM_{2.5}$ mass concentration and the construction sectors are also considered an important source of particle mass (Guttikunda et al., 2014; Butt et al., 2016; Conibear et al., 2018). Furthermore, it is particularly important to understand the absolute contribution and sources of different sizes of particles within $PM_{2.5}$. A recently published paper by Das et al. (2021) highlighted that <250 nm particles contribute a significant proportion of the total $PM_{2.5}$ mass and are a potentially important link with human health.

The Particle Number Size Distribution (PNSD) can provide air pollution source apportionment with high time resolution compared to use of chemical species, and influences the aerosol transport and transformation profiles in the urban atmosphere and toxicological effects on humans (Wu and Boor, 2021). Many PNSD studies have been conducted in urban, traffic and background sites over the past decades and three review studies have been published (Vu et al., 2015; Azimi et al., 2014; Wu and Boor, 2021). There are some studies evaluating the number or mass particle size distribution (PSD) in Delhi (Mönkkönen et al., 2005; Chelani et al., 2010; Gupta et al., 2011; Pant et al., 2016; Gani et al., 2020). Harrison (2020) compared PNSDs from Delhi, Beijing and London and reported that the particles from Delhi are far greater in number with a much larger modal diameter, close to 100 nm. In a recent paper, Gani et al. (2020) has investigated the PNSD up to 0.5 µm sizes from 2017 to 2018 and reported that rapid coagulation is an important process in Delhi.

The wide range PNSD is important to describe all sources of inhalable particles (<10 µm). It is not easy to separately identify particles arising from resuspension, sea salt and construction, or from brake wear and combustion or vehicle exhaust, using only the <0.5 µm particle size range. Harrison et al. 2011 reported that using wide range particle sizes in source apportionment was extremely successful in identifying the separate contributions of on-road emission including brake wear and resuspension. Although there are a few studies of wide range particle characterization in Beijing (Jing et al., 2014)

and source apportionment in Venice, Italy (Masiol et al., 2016), there has been no previous wide range PNSD study in Delhi. In this study, we aimed to interpret particulate matter size distributions over a wide range (15 nm to 10 µm) in the winter, post-monsoon and pre-monsoon seasons in Delhi. Future studies will look at two-step receptor modelling of wide range particulate matter size distributions and chemical composition in Delhi.

2. METHODS

2.1 Study Area

The measurements were part of the NERC/MoES Air Pollution and Human Health in an Indian mega-city (APHH-Delhi, www.urbanair-india.org) study, a joint UK-India project addressing air pollution in Delhi. The sampling location was ~15 m above ground level on the 5th floor of the Civil Engineering Department at the Indian Institute of Technology Delhi (IIT Delhi) campus, located in New Delhi, representative of an urban background environment (28.545 N, 77.193 E) (Figure S1). The measurement station is at a 120 m distance from a major arterial road. As part of APHH-Delhi, there were three field campaigns: (i) Jan-Feb 2018 (winter), (ii) May-June 2018 (summer; pre-monsoon) and (iii) Oct-Nov 2018 (autumn; post-monsoon). In all field campaigns, a suite of gas and particulate phase instrumentation was deployed within a temperature controlled laboratory.

These sampling periods were representative of conditions for PM and gases during these seasons in Delhi. We found the average $PM_{2.5}$ concentration to be approximately 180 µg/m^3, 220 µg/m^3 and 120 µg/m^3 for winter, autumn (excluding Diwali) and summer, respectively measured by a TEOM-FDMS (TEOM-Filter Dynamic Measurement System). Hama et al. (2020) studied the long term (from 2014 to 2017) trends of air pollution in Delhi at 6 stations (residential, commercial, and industrial sites) and reported that the mean $PM_{2.5}$ concentrations ranged between 147 – 248 µg/m^3, 147 – 248 µg/m^3 and 76 – 135 µg/m^3 for winter, autumn and summer, respectively, and a good correlation between

sites within Delhi. This gives reassurance that the $PM_{2.5}$ concentrations measured at our site are within the typical range of those observed in Delhi.

2.2 Measurements

Aerosol particle sizes in the atmosphere span a very wide range from a few nanometers at the lower end to some tens of micrometers at the upper end. Because of this very wide range of sizes, particle properties vary considerably across the size spectrum with the behaviour of the smaller particles being determined by their high mobility and hence diffusivity, whilst at the coarse end of the size distribution inertial properties are especially important. Due to this divergence in behaviour, no instrument is capable of measurement of the whole range of particle sizes.

To measure the particle size range used in this study, two particle instruments were used to collect number size distributions (NSD). For the range 15-640nm, a TSI- Scanning Mobility Particle Sizer (SMPS) 3936 was used, consisting of a TSI 3080 Electrostatic Classifier, TSI 3081 DMA and TSI 3775 CPC. To extend this range into the coarse mode a Portable Laser Aerosol Spectrometer and Dust Monitor (GRIMM 1.108) were used alongside the SMPS.

2.3 Merging Process

Merging procedures have usually been reported for merging SMPS and APS (Aerosol Particle Sizer) data, but here Grimm optical spectrometer (OP) data is merged with SMPS data. For a complete particle size distribution, simultaneously collected, paired hourly averaged particle number size distributions collected from the SMPS and Grimm were merged. The merging procedure is based on the principle of converting the diameters of the Grimm-derived data to a diameter matching the SMPS-derived data, in the region where the size distribution measurements overlap. The Grimm measures the optical diameter d_b^t whereas the SMPS measures the mobility diameter d_a^t of the particles. Comprehensive descriptions of the procedure and mathematics are given by DeCarlo et al. (2004) and Schmid et al. (2007). The Grimm NSD are translated onto the extended electical mobility

diameter axis of the SMPS using equation (R1) (Beddows et al. 2010; Liu et al., 2016; Ondracek et al., 2009).

$$d_b^t = \frac{d_a^t}{X}\sqrt{\frac{C(d_a^t)}{C(d_b^t)}} \quad \text{(R1)}$$

The Cunningham slip correction factor is given by C and the unknown variables such as the shape factor of the particles are accounted for by a free parameter X (given by equation R2) which is adjusted until the tails of the SMPS and Grimm NSD overlap each other giving a continuous NSD across the particle size bins measured by the two instruments.

$$X = \sqrt{\frac{\rho_e^t}{\rho_o}} \quad \text{(R2)}$$

The estimated transition-regime effective density ρ_e^t (normalised by the unit density, ρ_o) typically ranges from 0.77 to 2.56 g/cm^3 when aerodynamic diameter is used in merging. Detailed information upon the effective particle density based on the geographical regions is seen in the Wu and Boor (2021) study.

The merging algorithm (originally programmed in CRAN R) was implemented using Excel spreadsheets and the solver tool minimised the separation between the tails of the overlapping SMPS and Grimm. Due to the imperfect nature of the data, each of the merges was allocated a factor indicating quality based on whether: (i) there is a successful fit; (ii) the scatter of the data across the overlapping tails; (iii) the fraction of points on the tail falling onto the fitted curve; and (iv) how smooth the overlap is (Table S1). The size bins overlap (300-700 nm) between Grimm and SMPS. This process was repeated for the winter, summer and autumn data sets and any results failing the test

were either repeated or the data removed from the analysis. In all, only 8 samples from 1117 failed to give an acceptable fit in the merge procedure.

2.4 Data and Quality Management

Data from SMPS and Grimm were measured with 1-min resolutionand converted to hourly averages. The seasons were categorized as winter, autumn and summer. The measurements were taken in winter from 12 January 16:00 to 11 February 04:00, in autumn from 24 October 16:00 to 11 November 10:00, in summer 16 May 19:00 to 05 June 15:00 in 2018. There were 709, 403 and 477 total pairs (hours) in the data sets in winter, autumn and summer, respectively. But 172, 43 and 257 pairs in winter, autumn and summer, respectively were excluded because of the non-availability of data at that time. Data coverage is 76 % for winter, 95 % for autumn and 46 % for summer. Figure S2 in the Supplementary shows hourly mean values of total particle counts for three seasons. In order to evaluate day and night time PNC (particle number concentration) differences, the day and night were defined as 07:00-19:00 and 19:00 – 07:00, respectively. All times reported are local times recorded in Indian Standard Time (IST; GMT+05:30).

R version 3.1.2 was used to analyse the data (R Core Team, 2015). Firstly, all data were checked for clean-up of the robustness of the data sets, to detect anomalous records and take out the extreme values. Data greater than the 99.5^{th} percentile were deleted. Diwali time in 2018 (7th of November 2018 from 16:00 to 23:00) was taken out the date set in order to exclude its extreme effect on PNSD values. Particle number concentrations during Diwali time are given in the Supplementary, Figure S3. There were some single gaps in the data matrixes. These missing data were replaced by linearly interpolated values from the nearest bins to those samples.

In the literature, PNCs measured below 1 µm are frequently split into three ranges: nucleation, Aitken and accumulation (Gani et al., 2020). Nucleation size ranges have variously been described as below

30 nm (Masiol et al. 2016) or below 25 nm (Gani et al., 2020) or below 20 nm (Wu and Boor, 2021). Some studies have evaluated wide range PNSDs split into 4 ranges (nucleation, Aitken, accumulation and coarse) (Masiol et al. 2016; Harrison et al., 2011). In this study, the modes have been aggregated into five size groups: nucleation (15-20 nm), Aitken (20 -100 nm), accumulation (100 nm – 1 µm), large fine (1 µm – 2.5 µm) and coarse (2.5 µm – 10 µm) based on merged. Ultrafine particles (UFP) are considered to be total PN counts of Nucleation and Aitken modes (<100 nm).

The particle mass was calculated for the SMPS+OP merged data, assuming a density of 1.6 g cm^{-3} (Gani et al., 2020). Estimation of particle density as a function of size is extremely difficult, and there are few data for particle density from Delhi. Since Gani et al (2020) used the density of PM at the same location as in our study, we used the same density value to convert PN to PM mass. Figure S4 shows the comparison of $PM_{2.5}$ measured by SMPS+OP and TEOM-FDMS in Delhi for the three seasons. Figure S5 shows the comparison of $PM_{2.5}$ with relative humidity measured by SMPS+OP and TEOM in Delhi for the three seasons. A good correlation of the estimated particle mass with independent measurements with a co-located TEOM-FDMS was observed, except in summer.

The cumulative frequency of observations as a function of particle size was calculated for each hour of the day. Standard central measures from the cumulative frequency plots were represented by the geometric mean diameter (GMD) for each size distribution. They were used to examine particle growth processes. Firstly, the growth of GMD was estimated visually from the diurnal GMD data plot (Fig. 8). The minimum growth time used for estimation of the growth rate (GR) was selected as three hours, and if the growth lasted for long enough, the GR was estimated. The observed growth of the GMD of the particle was quantified by fitting the GMD of particles during the growth process event over a period of time 't' (euation R3~~q.1~~). Detailed information on the method can be found in Sarangi et al. (2015; 2018).

Growth rates (nm/hour)-GR =dGMD/dt (R31)

3. RESULTS

3.1 Particle Number and Size

Table S2 gives the descriptive statistics of particle number counts (#/cm^3) calculated using every 1-hour measurements for the nucleation, Aitken, accumulation, large fine and coarse modes between 15 nm and 10 µm in all seasons. Time series of total particle number counts are presented in Figure S2. The average total PN levels were 36.73x10^3 cm^{-3} in winter, 29.35x10^3 cm^{-3} in autumn and 18.91x10^3 cm^{-3} in summer. Generally, the wintertime PN levels were higher than the other seasons. The wintertime PN levels of nucleation, Aitken and accumulation modes were ~1.5, 1.8 and 2.2 times higher than in summer, respectively. Similar ratios were obtained by Guttikunda and Gurjar (2012) in Delhi for particulate matter concentrations. This is attributed to the unfavorable dispersion conditions, including low wind speed and low mixing height during the winter season. The autumn PN levels of nucleation, Aitken and accumulation modes were ~1.5, 1.3 and 1.9 times higher than in summer, respectively. The wintertime and autumn average PN levels are similar except for the Aitken mode for which winter is 1.4 times higher than in autumn. However, for the large fine and coarse modes the PN level was not markedly different between winter, autumn, and summer. Gani et al. (2020) reported that the average PN levels were 52.50 x10^3 cm^{-3} in winter, 43.40x10^3 cm^{-3} in summer, and 38.00x10^3 cm^{-3} in autumn in Delhi measured in 2017. The differences in the magnitude of number counts between the two studies are potentially explained by the difference in the sampling period and changes in emissions.

Figure 1 shows a comparison of average particle number and volume and the contribution to total PN. The average PV (particle volume) levels indicate that PV of the Aitken mode is highest in winter, while the accumulation mode is highest in autumn and the coarse mode is highest in summer. The contribution of UFP to numbers is highest in summer (57 %) but their contribution to volume is the lowest in autumn and summer (<1 %). The contribution to both number and volume of the

accumulation mode is highest in autumn with 51 % and 75 %, respectively. UFP contributions to total PV are below 1 % in Delhi. Furthermore, it can be seen clearly that the coarse fraction of particles dominates in summer, while the accumulation mode dominates in autumn and winter.

Wu and Boor (2021) analysed the PNSD observations made between 1998 and 2017 in 114 cities in 43 countries around the globe. They reported that there are significant variations in the magnitude of urban aerosol PNSD among different geographical regions. The main finding of their study is that the PNSD in Europe, North America, Australia, and New Zealand are dominated by nucleation- and Aitken-mode particles while in Central, South, Southeast and East Asia they are dominated by the substantial contribution from the accumulation mode, which is consistent with our finding. Pant et al. (2016) report mass size distributions for particulate matter sampled by cascade impactor in Delhi in winter. The dominant modes appear at around 3-4 µm and 0.6 µm, with a lesser peak at 0.2 µm aerodynamic diameter. These are respectively in the coarse (former mode) and accumulation (latter two modes) ranges as classified in the current study. The largest component of mass was in the accumulation mode, and the distribution fits well with the pattern of data seen in Figure 1. Major components of the coarse fraction were Al, Si, Ca and Fe (Pant et al., 2016), suggestive of soil and street dust as major contributors. The elements most notably in the accumulation fraction were Cu, Zn, Pb and Sb, indicative of non-exhaust traffic emissions and metallurgical sources, and S, which showed a major peak due to sulphate, peaking at 0.9 µm (Pant et al., 2016).

3.2 Diurnal Change

Figure 2 shows the diurnal variation of particle number concentrations and of $PM_{2.5}$, BC, NO and NO_2 for each season (excluding the day of Diwali), and the normalized time variations of all particle fractions are given in Figure S6. Figure S7 represents the diurnal variation of meteorological parameters. In general, there are large differences of PN levels between cold seasons (winter and autumn) and warm season (summer) for nucleation size particles. Coarse mode particle numbers in

the summer are higher than in winter and autumn, except in the evening time. For autumn and winter, particle counts are similar from 7 am to 7 pm (daytime). However, from 7 pm to 7 am particle counts in winter are higher than in autumn. The lowest levels for all modes were present during the afternoon in all seasons (2-4 pm), followed by highest levels during the night in winter (after 8 pm). The winter and autumn diurnal profiles had two peaks for below 1 μm particle size in the morning and evening corresponding to the traffic rush hours. But in the summer the same peaks for nucleation, Aitken and accumulation modes are seen although of smaller magnitude, and one hour earlier comparing to the winter and autumn. Pant et al. (2016) reported the diurnal variation of traffic at one of the major arterial roads in Delhi and Dhyani et al. (2019) reported on traffic-related emission. Figure S9 shows the diurnal variation in traffic at a major road intersection in Delhi. Cars, two/three wheelers, bus and LCV (light commercial vehicle) fleet numbers increase in the morning, persist throughout daytime and start to decrease at 22:00. Due to the prohibition of access for heavy-duty diesel vehicles to central Delhi from 6:00 am until 11:00 pm in the night, during the daytime including the traffic rush hours the HCV (heavy commercial vehicles) number is at its lowest level (Figure S9 or Dhyani et al. 2019). While road traffic clearly influences the diurnal pattern in PN, other sources including cooking and domestic combustion are likely to contribute. Small midday PN peaks were observed during the summer in the nucleation, Aitken and coarse modes. Another study conducted in Delhi reported the same midday peaks in the warm season and the highest levels in the cold season (Gani et al. 2020), which may be related to bus and LCV emissions at midday.

Figure 3 shows the differences in diurnal variations of total PN levels between the weekday and weekend. These are based upon a small dataset, and hence the rather small differences within a season may not be meaningful. In winter the PN levels on Saturday and Sunday are higher than on the weekdays during the night (from 8 pm to 10 am the next day). However, after the morning rush hour peaks, during the daytime the PN levels are the same for all days. The diurnal variation of PN in the autumn shows no significant differences among the days with the same main peaks in the morning

for all days, although highest on Saturday. There is a flattened peak (from 8 to 10 am) in the morning rush hour for the weekday while there are pointed peaks at approximately 9 am on Saturday and Sunday in winter and autumn. Measurements made during the summer period are very limited. Due to there being only 4 full days and 9 half days of measurements, it is very hard to draw any conclusions. Even so, there are indications of a weekday traffic effect upon the PN levels in summer. There is only one day of measurements on a Sunday (3rd June 2018) and it shows the midday peaks. Overall, despite seasonal differences, there appears to be a strong influence of light duty road vehicles upon the diurnal profiles, reflecting traffic volumes, with an impact of heavy duty vehicles upon nighttime concentrations of all particle fractions.

NPF events present variable seasonality for different areas, though in most cases they appear to be more frequent during spring or summer (Salvador et al., 2021). Gani et al. 2020 studied long term PNSD in Delhi and have stated that they did not see any NPF during the winter or autumn seasons in Delhi. In this study, the identification of NPF events was conducted manually using the criteria set by Dal Maso et al. (2005) and used by Bousiotis et al (2019; 2021). The data were analysed visually on a day-to-day basis: each 24-hour period, from midnight to midnight. According to these criteria, a NPF event is considered when: a distinctly new mode of particles appears in the nucleation mode size range, prevails for some hours, and shows signs of growth. These are the initial criteria used in identifying the events. Following that, as the dataset starts from a rather large size (15 nm), to be more confident about the events and not to confuse them with pollution events, high time resolution data for NO_x as well as the fluctuations of the condensation sink were also used to identify pollution events affecting particle concentrations which were not considered. Hence, while we checked the particle size distributions for the NPF events, we also looked at the levels of pollutants to ensure that what was attributed to a NPF event was not particles from pollution / direct emissions. By considering the pollution levels and condensation sink we can reduce the possibility of including particle formation events that are not associated with secondary formation. After analysing all data,

measurements from only one day during the measurement campaign were compliant with the criteria set as a class Ia NPF event. Figure 4 presents the contour plots of average diurnal variation for all seasons and for the NPF event on 3rd June. NPF may be suppressed due to very high pre-existing aerosol concentrations (Kanawade et al., 2020; Gani et al. 2020) during severe air pollution episodes in Delhi. This suppression effect has also been observed in European cities (Bousiotis et al., 2019; 2021).

A new study by Sebastian et al. (2021) analysed PNSD and the frequency of NPF at six different locations in India. The Delhi observation site is in an urban area and located at CSIR-National Physical Laboratory (NPL), approximately 8 km from the IIT location described as urban background in our study. They found that the NPF frequently occurs in the spring season, but is least common in autumn and winter due to air pollution episodes suppressing the NPF. They also stated that the highest concentration and frequency of occurrence of NPF events in was Delhi as compared to other sites. As in other studies (such as Bousiotis et al., 2021), this study also emphasized that the increased concentrations of precursor gases are important for the occurrence of NPF in urban areas.

3.3 Day and Night Time Differences in PN and PV

Table S3 presents the summary statistics of the particle number and mass levels derived from merged particle number data and BC, NO_x and $PM_{2.5}$ at night and day for each season, excluding Diwali. Figure 5 shows the particle number comparison of all modes at night and day seasonally. In both night and day, the nucleation counts are approximately the same in autumn and summer (N/D=1.1 and 1.0), and a little higher at night in winter (N/D=1.3). But in the night, Aitken and accumulation counts are higher than in the day by factors of 1.4 and 1.5 times in summer, 1.2 and 1.5 times in autumn, respectively and approximately 2 in winter. While the coarse mode PN counts are approximately the same for all seasons and day / night, the large fine PN level in the nighttime are significantly higher (1.7) than in the daytime in summer. It seems that in the nighttime high PM concentrations are due to the increasing Aitken and accumulation modes occurring from coagulation

of nucleation mode particles, condensation of low volatility species or hygroscopic growth. In addition, biomass burning and older diesel vehicles can contribute significantly to particles in these fractions (Kumar et al., 2013; Chen et al., 2017; Gani et al., 2020). Meteorological factors can also profoundly affect the PN levels in daytime and nighttime. The differences of wind speed between day and night in summer are lower than in winter and autumn (Figure S7). Higher wind speed, and lower humidity, may favour the resuspension of coarse dust as a dominant mechanism in the summer. Seasonal changes in mixing depths are surprisingly small (Figure S7) and hence unlikely to have a major influence. However, the major increases and decreases in the diurnal plots of pollutants (Figure 2) are consistent with the diurnal plots of MLH (Figure S7). Autumn and winter also have longer periods with low mixing heights, also seen in Figure S7. TPN showed a negative exponential dependence upon MLH, which became more scattered at lower values of MLH, probably reflecting the larger relative errors in MLH estimates at smaller values.

Figure S8 represents the relation between the ventilation coefficients (VC = MLH × wind speed) and TPN as a function of hour and month. Gani et al. (2019) reported that the VC is 4–6 times smaller for the wintertime compared to the summer in Delhi. In this study, the VC is 1.8 and 1.6 times higher in summer (mean 2732 m^2/s) compared to the winter (mean 1491 m^2/s) and autumn (mean 1702 m^2/s), respectively. The daytime hourly TPN levels are lower as related to the higher VC and the lower VC in colder months gives higher TPN. Although there are not enough daily data (especially for summer) to give more detail, we can see the same trend as comparing to the weekly data from Gani et al (2019) study.

Overall, for the daytime for all seasons, hourly averaged UFP concentrations are usually less than the nighttime, however the UFP contribution to the PN_1 (55 % in day, 50 % in night for winter; 52 % in day, 45 % in night for autumn; 58 % in day, 56 % in night for summer) and PN_{10} (38 % in day, 38 % in night for winter; 40 % in day, 33 % in night for autumn; 36 % in day, 33 % in night for

summer) are mostly slightly higher in the daytime. Similarly, Gani et al. (2020) have reported the highest contribution (of UFP to PNC) in the daytime compared with the nighttime in Delhi. Due to the difference of PN size range (they measured down to 12nm), they found the UFP contribution to PNC higher than in the present study.

3.4 Size Distributions

Figure 6 shows the average PNSD in three seasons in Delhi. Volume and Area distributions are shown in the Supplementary Materials in Figure S10. The highest number concentrations are seen in winter, followed by autumn, and then summer. Although the number concentrations of particles below 200 nm are far greater in winter those between 200 and 600nm are greater in autumn, within the accumulation mode. The winter and summer PNSD show modes at approximately 100 nm but the autumn PNSD shows the mode at approximately 200 nm. This could be due to changing sources of particles in Delhi between seasons (Jain et al. 2020), in addition to (differing) aerosol dynamical processes. The Delhi atmosphere is more polluted comparing with most other cities based on particle number and mass (Harrison, 2020). This will cause a tendency for particles to grow more rapidly by coagulation and condensation (Harrison et al., 2018), but this might be expected to occur in all seasons.

As described above, in Delhi the nighttime particle concentrations are markedly higher than the daytime concentrations. The PNSD changes for each hour of the day across all three seasons were analysed (Figure S11) and categorized. Figure 7 presents the PNSD differences between daytime and nighttime and shows the variation in PNSDs within the day in all seasons. The main difference between day and night in winter is only the number concentration, with little change in the mode size between day and night, while the PNSDs in summer and autumn show bimodal distributions with modes at approximately 30 and 140 nm in summer, and 35 and 200 nm in autumn. When we focus on PNSD during the daytime, it can be clearly seen that the modes are manifest at different times: In

winter, while the PNSD shows the same mode at approximately 100 nm from 8 am to 2 pm, the mode in the afternoon (from 2 pm to 6 pm) drops slightly in size (70 nm). In the morning and afternoon there are two small peaks at 60 nm and 40 nm for the Aitken fraction and 170 and 130 nm for the accumulation fraction in autumn. During the day in summer, there are two peaks at approximately 30 nm from 10 am to 6 pm. This may be associated with summer nucleation events and NPF on 3rd June 2018 (Figure 4). Furthermore it may be related to the growth of particles from 10 am to 2 pm in autumn and summer. The full reasons for these changing PNSDs are not clear, and it would be unwise to attempt a detailed interpretationof a very small dataset.

Figure 8 shows the average geometric mean diameter (GMD) change with hour of the day. Two overall periods of GMD increase are observed. One of them is in nighttime in all seasons with GMD growing at between 4.6 nm/hour in summer and 6.2 nm/hour in winter. The particle growth in autumn is predominantly (when compared to the winter and summer) both late in the night (from 0 am to 5 am) and in the morning (from 8 am to 12 pm). Considering the PNSD trend in autumn (Figure 7), the GMD rises at 9 nm/hour from morning to noon. Similar results were obtained in the USA (Kuang et al., 2012), Canada (Jeong et al., 2010; Iida et al. 2008), Italy (Hamed et al., 2007) and Japan (Han et al. 2013). However the calculated GMD growth rate is smaller than that calculated by Sarangi et al., (2015; 2018) in Delhi, by Kalafut-Pettibone et al. (2011) in Mexico City and by Zhang et al. (2011) in Beijing. The changing GMD with time in Delhi could be the result of changing sources, and/or of dynamics. Nocturnal growth may be the result of reducing temperatures and increasing RH causing vapour condensation (Sarangi et al., 2018). Morning growth may be due to oxidation processes leading to production of less volatile vapours which then condense onto the particles (Sarangi et al. 2018).

Figure 9 gives the average particle number, volume, area and mass size distribution for all seasons. While the number size distributions have one mode, two peaks are observed in volume distributions,

centered at 0.5 µm and 6 µm. These relate to two different main sources, which might be secondary aerosol (such as sulphate at high RH) in the fine mode and road dust resuspension, soil or construction dust for the coarse mode (Pant et al. 2016). In winter and autumn fine mode particle volumes are higher than the coarse mode. However, in summer the coarse mode particle volumes are higher than the fine particle level. In a recent paper, Thamban et al. (2021) show that modes in the mass size distributions of hydrocarbon organic aerosol (HOA), Semi-volatile oxygenated organic aerosol (SVOOA), biomass burning organic aerosol (BBOA) and low-volatile oxygenated organic aerosol (LVOOA) measured by aerosol mass spectrometry are typically in the range 300-600nm vacuum aerodynamic diameter, very consistent with the peaks seen in the mass distributions in Figure 9.

Hama et al. (2020) obtained the spatiotemporal characteristics of daily-averaged air pollutants and concluded that the particulate matter mass (PM_{10} and $PM_{2.5}$) is dominated by local sources across Delhi. The main local air pollutant sources in Delhi include traffic, construction, resuspension of dust, diesel generators, power plants, industries and biomass burning (Kumar et al., 2013; Nagpure et al., 2015; Hama et al., 2020).

All average PNSD graphs show an increasing trend in PNC at particle sizes below 19 nm particle diameter. SMPS measurements in this study were conducted only above 15 nm. So, the peak particle size within this size range cannot be seen. However, the clear increase in particle number below 19 nm indicates that another source may be important in Delhi. This small mode and bimodal PNSD during the day (Figure 7) may be associated with the road transport vehicle types in Delhi. Despite the diesel restriction during the rush hours and conversion of the public transport vehicles to CNG, several studies have reported that $PM_{2.5}$ concentrations have been remaining steady or are slowly increasing in India, especially in the winter and autumn seasons (Babu et al., 2013; Balakrishnan et al., 2019; Dandona et al. 2017; Kumar et al., 2017).

The fuels used in Delhi's traffic fleet are petrol, diesel, CNG and LPG. Legislation limits the sulphur content of the fuel to 50 ppm in diesel as per Bharat Stage IV. The diesel vehicles are not required to be fitted with particle traps. The technology of the gasoline vehicle fleet varies as vehicle engine capacity changes. Cars, two/three wheelers, bus and LCV fleet volumes are high during the day. Due to the time restrictions on trucks/heavy good vehicles entering the city, during the daytime the HCV number is at its lowest level (Figure S9).

Previous published studies indicate that emissions of particles from CNG vehicles (Euro 4, 5, 6) with diameter greater than 23 nm are as low as a diesel particle filter equipped vehicle, and an order of magnitude lower than gasoline vehicles (Kontses et al. 2020; Giechaskiel, et al. 2019; Magara-Gomez et al. 2014; Schreiber et al. 2007), and CNG vehicles mainly emit nuclei-mode particles (Zhu et a., 2014; Toumasatos et al. (2020). Zhu et al. (2014) calculated size-resolved particle emission factors from on-road diesel buses and CNG buses and reported that the PNSD of diesel buses dominate the accumulation mode diameters of 74-87 nm while the PNSD of CNG buses dominated the nucleation mode with modes at 21-24 nm. Total PN emissions of diesel buses per vehicle were 4 times higher than the level of CNG buses. However, the PN level in the nucleation mode (15-25 nm) of CNG buses was 1.7 times higher than from the diesel buses in the nucleation mode. Toumasatos et al. (2020) studied the particle emission performance of the Euro 6 CNG and gasoline vehicles and discussed the current EU cut-off solid PN size threshold of 23 nm. The results revealed that PN>23 nm represented 43 % of PN>10 nm and 8 % of PN>2.5 nm for gasoline vehicles and 7 % of PN>10 nm and 1 % of PN>2.5 nm for CNG vehicles respectively. These studies of emission PNSDs show that a significant number of particles reside below the EU lower measurement limit of of 23 nm, and many are even smaller than 10 nm. These probably contribute to the mode seen just appearing at the extreme small particle limit of Figure 9.

When the PNSD results measured in Delhi are compared with the main emission categories in the literature (Kumar et al., 2013; Vu et al., 2015), it seems that the average size distributions measured in the atmosphere in Delhi are much coarser, which is presumably due to condensation and coagulation, or it could be that secondary particles dominate over the primary emissions. Pant et al. (2016) hypothesised that the main accumulation mode peak in their winter measurements arose from aqueous droplet evaporation, although this mechanism would be unlikely to explain the mode seen in the summer data. Thamban et al. (2021) have also reported particle growth in the Delhi atmosphere from condensation of organic compounds formed from oxidation processes.

Previous studies have attempted to quantify the relative contribution of primary and secondary sources to the total and mode-segregated particle number concentrations (Kulmala et al. 2021; Casquero-Vera et al. 2021; Hama et al. 2017; Kulmala et al. 2016; Rodríguez, & Cuevas, 2007). Rodríguez and Cuevas (2007) first presented the methodology for the separation of traffic related primary aerosol particles from the total using the BC as the main tracer of traffic. The method was tested in this study, but did not prove appropriate as the BC sources in Delhi are more complex, and arise not only from traffic. The BC diurnal trend (Figure 2) does not show the rush hour peaks, and reflects mostly the combustion activity at night, presumably including the heavy duty diesel emissions. A recent study by Kulmala et al. (2021) used NO_x as a tracer of primary sources. Figure 2 shows that only the NO_2 diurnal trend in autumn is clearly related to traffic sources. Furthermore the sources of BC and NO_x are largely the same, as judged from the high similarity between BC and NO_x diurnal trends (Figure 2).

3.5 Correlations of PN with NO_2, NO, and BC

Figure 10 shows the correlation coefficients between the hourly average PNs of five particle size fractions and NO, NO_2, and BC measured in Delhi. Nucleation mode PN is better correlated with the Aitken mode PN in winter and summer despite the lower correlation in autumn. The correlations

among >1 μm size fractions are higher in summer than winter and autumn. Tyagi et al. (2016) stated that the major source of NO_x emissions is vehicle exhaust and power plants in Delhi. Furthermore, studies have reported that approximately 80-90 % of NO_x and CO are produced from the transport sector in Delhi (Gurjar et al., 2004; Gulia et al., 2015; Tyagi et al., 2016; Hama et al., 2020). As seen in Figure 2, the NO_2 diurnal trend is very similar to nucleation and Aitken particle trends, especially in the autumn. NO_2 peaks in autumn in the traffic rush hours are larger than in winter and summer. In addition, there are no significant correlations between NO_2 and NO or BC in autumn (0.02 for NO, 0.03 for BC) compared to the summer (0.73 for NO, 0.61 for BC) and winter (0.37 for NO and 0.28 for BC) (Figure S12). NO and BC diurnal trends show the same higher level in the night (Figure 2) and also, they have higher correlation coefficients (0.78 in winter, 0.77 in summer, 0.72 in autumn) for all seasons, similar to the accumulation mode particle counts (Figure 2, Figure 10, Table S2). NO_2 and <100 nm particles may be associated with traffic sources, while the NO and BC and <1 μm particles could be associated with biomass burning, industry, (small generator) power generation, or possibly also with diesel vehicles.

3.6 Wind Effects

Figure S13 represents polar plots of BC, NO and NO_2 measured in Delhi. This shows no consistent pattern. There are differences between the pollutants in terms of directional and wind speed associations, and for each pollutant / season. There is no obvious indication of a strong local source influence, typically manifest as an intense area in the very centre of the plot circle. The plots for the particle size fractions (Figure 11) also show little consistency between seasons for a given size fraction. Within a season, however, adjacent size fractions often show a similarity of behaviour (consistent with their correlations, see above) but this similarity does not extend across all size ranges within a season.

4. CONCLUSIONS

This study serves to highlight the remarkable complexity of airborne particulate matter in Delhi. The size distributions show marked seasonal changes, with coarse particles dominant in summer, but not in the cooler seasons, when the accumulation mode dominates. The measured size distributions show a fine mode aerosol with a considerably larger modal diameter than that typically seen in western countries, and larger than the modal emission size from major source categories. It appears the that the high particle concentrations and chemically reactive atmosphere are promoting rapid coagulation and condensational growth of particles, and therefore the measured size distributions are driven more by aerosol dynamical processes than source characteristics. Growth via a liquid droplet phase in the cooler months may also occur. There is little evidence for a contribution of new particle formation (although the summer season dataset is small), consistent with earlier work by Gani et al. (2020). Another notable feature is the apparent complexity and seasonal variability of sources of NO, NO_2 and BC, pollutants which can often be used to identify or locate sources of emissions. This is reflected in the various particle fractions, which generally correlate poorly with the other pollutants and with other than proximate size fractions.

The diurnal variation of all particle fractions is strongly suggestive of a road traffic influence, especially in the winter campaign. This appears strongly influenced by the emissions of heavy duty diesel traffic which is only able to access central Delhi at night. A size mode of <15 nm may well be attributable to vehicles using LPG/CNG fuels. However, the seasonal variability of the geographic distribution and wind speed dependence of sources revealed by the polar plots is strongly indicative of many other sources also contributing to all size fractions of particles.

DATA ACCESSIBILITY

Data supporting this publication are openly available from the UBIRA eData repository at https://doi.org/10.25500/edata.bham.00000730

AUTHOR CONTRIBUTIONS

This study was conceived by RMH. WJB managed the research programme, and MSA and LRC collected the data. DCB and UAS led the data analysis with contributions from JB and DB. UAS and RMH co-authored the first draft. ZS and all co-authors provided comments and revisions.

COMPETING INTERESTS

The authors declare that they have no conflict of interest.

FINANCIAL SUPPORT

This research has been supported by the Natural Environment Research Council NE/P016499/1.

ACKNOWLEDGEMENTS

We are thankful the Scientific and Technical Research Council of Turkey (TUBITAK) (grant number 1059B191801445) to support the author Ulku Alver Sahin to work on the ASAP project. We would also like to acknowledgement the IIT Delhi team under the Principal Investigator-ship of Professor Mukesh Khare who provided all the facilities including space and logistical help during the experiment.

REFERENCES

Azimi, P., Zhao, D. and Stephens, B.: Estimates of HVAC filtration efficiency for fine and ultrafine particles of outdoor origin, Atmos. Environ., 98, 337-346, https://doi.org/10.1016/j.atmosenv.2014.09.007, 2014.

Babu, S. S., Manoj, M.R., Moorthy, K. K., Mukunda, M. G., Vijayakumar, S.N., Sobhan, K.K., Satheesh, S.K., Niranjan, K., Ramagopal, K., Bhuyan, P.K. and Singh, D.: Trends in aerosol optical depth over Indian region: Potential causes and impact indicators, J. Geophys. Res, 118, 11794–11806, https://doi.org/10.1002/2013JD020507, 2013.

Balakrishnan, K., Pillarisetti, A., Yamanashita, K. and Yusoff, K.: Air Pollution in Asia and the Pasific: Science Based Solution, Published by the United Nations Environment Programme (UNEP), Chapter 1.2 Air quality and health in Asia and the Pacific, January 2019, ISBN: 978-92-807-3725-7, Bangkok, Thailand, 2019.

Beddows, D. C. S., Dall'osto, M. and Harrison, R. M.: An Enhanced Procedure for the Merging of Atmospheric Particle Size Distribution Data Measured Using Electrical Mobility and Time-of-Flight Analysers, Aerosol Science and Technology, 44, 11, 930-938, https://doi.org/10.1080/02786826.2010.502159, 2010.

Bhandari, S., Gani, S., Patel, K., Wang, D. S., Soni, P., Arub, Z., Habib, G., Apte, J.S. and Ruiz, L. H.: Sources and atmospheric dynamics of organic aerosol in New Delhi, India: insights from receptor modeling, Atmos. Chem. Phys., 20, 735–752, https://doi.org/10.5194/acp-20-735-2020, 2020.

Bikkina, S., Andersson, A., Kirillova, E. N., Holmstrand, H., Tiwari, S., Srivastava, A. K., Bisht, D.S. and Gustafsson, Ö.: Air quality in megacity Delhi affected by countryside biomass burning, Nature Sustainability, 2, 200–205, https://doi.org/10.1038/s41893-019-0219-0, 2019.

Bousiotis, D., Dall'Osto, M., Beddows, D. C. S., Pope, F. D., and Harrison, R. M.: Analysis of new particle formation (NPF) events at nearby rural, urban background and urban roadside sites, Atmos. Chem. Phys., 19, 5679–5694, https://doi.org/10.5194/acp-19-5679-2019, 2019.

Bousiotis, D., Brean, J., Pope, F. D., Dall'Osto, M., Querol, X., Alastuey, A., Perez, N., Petäjä, T., Massling, A., Nøjgaard, J. K., Nordstrøm, C., Kouvarakis, G., Vratolis, S., Eleftheriadis, K., Niemi, J. V., Portin, H., Wiedensohler, A., Weinhold, K., Merkel, M., Tuch, T., and Harrison, R. M.: The effect of meteorological conditions and atmospheric composition in the occurrence and development of new particle formation (NPF) events in Europe, Atmos. Chem. Phys., 21, 3345–3370, https://doi.org/10.5194/acp-21-3345-2021, 2021.

Butt, E. W., Rap, A., Schmidt, A., Scott, C. E., Pringle, K. J., Reddington, C. L., Richards, N. A. D., Woodhouse, M. T., Ramirez-Villegas, J., Yang, H., Vakkari, V., Stone, E. A., Rupakheti, M., S. Praveen, P., G. van Zyl, P., P. Beukes, J., Josipovic, M., Mitchell, E. J. S., Sallu, S. M., Forster, P. M., and Spracklen, D. V.: The impact of residential combustion emissions on atmospheric aerosol, human health, and climate, Atmos. Chem. Phys., 16, 873–905, https://doi.org/10.5194/acp-16-873-2016, 2016.

Casquero-Vera, J. A., Lyamani, H., Titos, G., Minguillón, M. C., Dada, L., Alastuey, A., Querol, X., Petäjä, T., Olmo, F. J. and Alados-Arboledas, L.: Quantifying traffic, biomass burning and secondary source contributions to atmospheric particle number concentrations at urban and

suburban sites, Science of The Total Environment, 768, 145282, doi.org/10.1016/j.scitotenv.2021.145282, 2021.

Chelani, A. B., Gajghate, D. G., ChalapatiRao, C. V. and Devotta, S.: Particle Size Distribution in Ambient Air of Delhi and Its Statistical Analysis, Bull. Environ. Contam. Toxicol., 85, 22–27, https://doi.org/10.1007/s00128-010-0010-4, 2010.

Chen, F., Zhang, X., Zhu, X., Zhang, H., Gao, J. and Hopke, P. K.: Chemical Characteristics of PM2.5 during a 2016 Winter Haze Episode in Shijiazhuang, China. Aerosol Air Qual. Res., 17, 368-380, https://doi.org/10.4209/aaqr.2016.06.0274, 2017.

Chowdhury, S., Dey, S., Tripathi, S. N., Beig, G., Mishra, A. K. and Sharma, S.:" Traffic intervention" policy fails to mitigate air pollution in megacity Delhi, Environmental Science & Policy, 74, 8-13, https://doi.org/10.1016/j.envsci.2017.04.018, 2017.

Conibear, L., Butt, E. W., Knote, C., Arnold, S. R. and Spracklen, D. V.: Residential energy use emissions dominate health impacts from exposure to ambient particulate matter in Indi,. Nat. Commun., 9, 617, https://doi.org/10.1038/s41467-018-02986-7, 2018.

Cusworth, D. H., Mickley, L. J., Sulprizio, M. P., Liu, T., Marlier, M.E., DeFries, R. S., Guttikunda, S.K. and Gupta, P.: Quantifying the influence of agricultural fires in northwest India on urban air pollution in Delhi, India, Environ. Res. Lett., 13, 044018, https://doi.org/10.1088/1748-9326/aab303, 2018.

Dal Maso, M., Kulmala, M., Riipinen, I., Wagner, R., Hussein, T., Aalto, P. P. and Lehtinen, K. E. J.: Formation and growth of fresh atmospheric aerosols: eight years of aerosol size distribution data from SMEAR II, Hyytiala, Finland, Boreal Environmental Research 10, 323-336, 2005.

Dandona, L., Dandona, R., Kumar, G. A., Shukla, D. K., Paul, V. K., Balakrishnan, K., Prabhakaran, D., Tandon, N., Salvi, S., Dash, A. P., Nandakumar, A., Patel, V., Agarwal, S. K., Gupta, P. C., Dhaliwal, R. S., Mathur, P., Laxmaiah, A., Dhillon, P. K., Dey, S., Mathur, M. R., Afshin, A., Fitzmaurice, C., Gakidou, E., Gething, P., Hay, S.I., Kassebaum, N. J., Kyu, H., Lim, S. S., Naghavi, M., Roth, G. A., Stanaway, J. D., Whiteford, H., Chadha, V. K., Khaparde, S. D., Rao, R., Rade, K., Dewan, P., Furtado, M., Dutta, E., Varghese, C. M., Mehrotra, R., Jambulingam, P., Kaur, T., Sharma, M., Singh, S., Arora, R., Rasaily, R., Anjana, R. M., Mohan, V., Agrawal, A., Chopra, A., Mathew, A. J., Bhardwaj, D., Muraleedharan, P., Mutreja, P., Bienhoff, K., Glenn, S., Abdulkader, R. S., Aggarwal, A. N., Aggarwal, R., Albert, S., Ambekar, A., Arora, M., Bachani, D., Bavdekar, A., Beig, G., Bhansali, A., Bhargava, A., Bhatia, E., Camara, B., Christopher, D. J., Das, S. K., Dave, P. V., Dey, S., Ghoshal, A. G., Gopalakrishnan, N., Guleria, R., Gupta, R., Gupta, S. S., Gupta, T., Gupte, M. D., Gururaj, G., Harikrishnan, S., Iyer, V., Jain, S.K., Jeemon, P., Joshua, V., Kant, R., Kar, A., Kataki, A.C., Katoch, K., Khera, A., Kinra, S., Koul, P.A., Krishnan, A., Kumar, A., Kumar, R. K., Kumar, R., Kurpad, A., Ladusingh, L., Lodha, R., Mahesh, P. A., Malhotra, R., Mathai, M., Mavalankar, D., Mohan Bv, M., Mukhopadhyay, S., Murhekar, M., Murthy, G.V.S., Nair, S., Nair, S. A., Nanda, L., Nongmaithem, R. S., Oommen, A.M., Pandian, J.D., Pandya, S., Parameswaran, S., Pati, S., Prasad, K., Prasad, N., Purwar, M., Rahim, A., Raju, S., Ramji, S., Rangaswamy, T., Rath, G. K., Roy, A., Sabde, Y., Sachdeva, K. S., Sadhu, H., Sagar, R., Sankar, M. J., Sharma, R., Shet, A., Shirude, S., Shukla, R., Shukla, S. R., Singh, G., Singh, N. P., Singh, V., Sinha, A., Sinha, D. N., Srivastava, R. K., Srividya, A., Suri, V., Swaminathan, R., Sylaja, P. N., Tandale, B., Thakur, J. S., Thankappan, K.R., Thomas, N., Tripathy, S., Varghese, M., Varughese, S., Venkatesh, S., Venugopal, K., Vijayakumar, L., Xavier, D., Yajnik, C. S., Zachariah, G., Zodpey, S., Rao, J. V. R. P., Vos, T., Reddy, K. S., Murray, C. J. L. and Swaminathan, S.: Nations within a nation: variations in epidemiological transition across the states

of India, 1990-2016 in the global burden of disease study. The Lancet, 390, 10111, 2437-2460, https://doi.org/10.1016/S0140-6736(17)32804-0, 2017.

Das, A., Kumar, A., Habib, G. and Vivekanandan, P.: Insights on the biological role of ultrafine particles of size PM<0.25: A prospective study from New Delhi, Environmental Pollution, 268, Part B, 115638, https://doi.org/10.1016/j.envpol.2020.115638, 2021.

DeCarlo, P. F., Slowik, J. G., Worsnop, D. R., Davidovits, P. and Jimenez, J. L.: Particle Morphology and Density Characterization by Combined Mobility and Aerodynamic Diameter Measurements. Part 1: Theory, Aerosol Science and Technology, 38:12, 1185-1205, https://doi.org/10.1080/027868290903907, 2004.

Dhyani, R., Sharma, N. and Advani, M.: Estimation of Fuel Loss and Spatial-Temporal Dispersion of Vehicular Pollutants at a Signalized Intersection in Delhi City, India. WIT Transection on Ecology and the Environmen: Air Pollution 2019, WIT Press, 236, 233-247, ISBN: 978-1-78466-343-8, Editor: Passerini et al., 2019.

Dumka, U. C., Tiwari, S., Kaskaoutis, D. G., Soni, V. K., Safai, P. D. and Attri, S. D.: Aerosol and pollutant characteristics in Delhi during a winter research campaign, Environ. Sci. Pollut. Res., 26, 3771–3794. https://doi.org/10.1007/s11356-018-3885-y, 2019.

Gani S., Bhandari, S., Patel, K., Seraj, S., Soni, P., Arub, Z., Habib, G., Ruiz, L.H. and Apte, J.S.: Particle number concentrations and size distribution in a polluted megacity: the Delhi Aerosol Supersite study, Atmos. Chem. Phys., 20, 8533–8549, https://doi.org/10.5194/acp-20-8533-2020, 2020.

Giechaskiel, B., Lähde, T. and Drossinos, Y. Regulating particle number measurements from the tailpipe of light-duty vehicles: The next step?, Environmental Research, 172, 1-9, https://doi.org/10.1016/j.envres.2019.02.006, 2019.

Gulia, S., Shiva Nagendra, S.M., Khare, M. and Khanna, I.: Urban air quality management-A review, Atmospheric Pollution Research, 6, 2, 286-304, https://doi.org/10.5094/APR.2015.033, 2015.

Guo, H., Kota, S.H., Sahu, S.K., Hu, J., Ying, Q., Gao, A. and Zhang, H.: Source apportionment of PM2.5 in North India using source-oriented air quality models, Environmental Pollution, 231, 1, 426-436, https://doi.org/10.1016/j.envpol.2017.08.016, 2017.

Gupta, S., Kumar, K., Srivastava, A., Srivastava, A. and Jain, V. K.: Size distribution and source apportionment of polycyclic aromatic hydrocarbons (PAHs) in aerosol particle samples from the atmospheric environment of Delhi, India, Science of The Total Environment, 409, 22, 4674-4680, https://doi.org/10.1016/j.scitotenv.2011.08.008., 2011.

Gurjar, B. R., van Aardenne, J. A., Lelieveld, J. and Mohan, M.: Emission estimates and trends (1990–2000) for megacity Delhi and implications, Atmospheric Environment, 38, 33, 5663-5681, https://doi.org/10.1016/j.atmosenv.2004.05.057, 2004.

Guttikunda, S. K., Goel, R. and Pant, P.: Nature of air pollution, emission sources, and management in the Indian cities, Atmospheric Environment, 95, 501-510, https://doi.org/10.1016/j.atmosenv.2014.07.006, 2014.

Guttikunda, S.K. and Gurjar, B.R.: Role of meteorology in seasonality of air pollution in megacity Delhi, India, Environ. Monit. Assess., 184, 3199–3211. https://doi.org/10.1007/s10661-011-2182-8, 2012.

Hama, S.M.L., Kumar, P., Harrison, R.M., Bloss, W.J., Khare, M., Mishra, S., Namdeo, A., Sokhi, R., Goodman, P. and Sharma, C.: Four-year assessment of ambient particulate matter and trace gases in the Delhi-NCR region of India, Sustainable Cities and Society, 54, 102003, https://doi.org/10.1016/j.scs.2019.102003, 2020.

Hama, S.M.L., Cordell, R. L. and Monks, P. S.: Quantifying primary and secondary source contributions to ultrafine particles in the UK urban background, Atmos. Environ., 166, 62-78, doi.org/10.1016/j.atmosenv.2017.07.013, 2017.

Hamed, A., Joutsensaari, J., Mikkonen, S., Sogacheva, L., Dal Maso, M., Kulmala, M., Cavalli, F., Fuzzi, S., Facchini, M. C., Decesari, S., Mircea, M., Lehtinen, K. E. J., and Laaksonen, A.: Nucleation and growth of new particles in Po Valley, Italy, Atmos. Chem. Phys., 7, 355–376, https://doi.org/10.5194/acp-7-355-2007, 2007.

Han, Y., Iwamoto, Y., Nakayama, T., Kawamura, K., Hussein, T. and Mochida, M.: Observation of new particle formation over a mid-latitude forest facing the North Pacific, Atmos. Environ., 64, 77-84, https://doi.org/10.1016/j.atmosenv.2012.09.036, 2013.

Harrison RM.: Airborne particulate matter, Phil. Trans. R. Soc. A, 378, 20190319. http://dx.doi.org/10.1098/rsta.2019.0319, 2020.

Harrison, R. M., Rob MacKenzie, A., Xu, H., Alam, M. S., Nikolova, I., Zhong, J., ... and Liang, Z., Diesel exhaust nanoparticles and their behaviour in the atmosphere. Proceedings of the Royal Society A, 474(2220), 20180492, 2018.

Harrison, R. M., Beddows, D.C.S. and Dall'Osto, M.: PMF Analysis of Wide-Range Particle Size Spectra Collected on a Major Highway, Environ. Sci. Technol., 45, 13, 5522–5528, https://doi.org/10.1021/es2006622, 2011.

Jain, S., Sharma, S. K., Vijayan, N., Mandal, T. K.: Seasonal characteristics of aerosols (PM2.5 and PM10) and their source apportionment using PMF: A four year study over Delhi, India, Environmental Pollution, 262, 114337, https://doi.org/10.1016/j.envpol.2020.114337, 2020.

Jeong, C.H., Evans, G. J., McGuire, M. L., Chang, R. Y.W. and Abbatt, J. P. D.: Zeromskiene, K., Mozurkewich, M., Li, S.-M., and Leaitch, W. R.: Particle formation and growth at five rural and urban sites, Atmos. Chem. Phys., 10, 7979–7995, https://doi.org/10.5194/acp-10-7979-2010, 2010.

Jing, H., Li, Y.F., Zhao, J., Li, B., Sun, J., Chen, R., Gao, Y. and Chen, C.: Wide-range particle characterization and elemental concentration in Beijing aerosol during the 2013 Spring Festival, Environmental Pollution, 192, 204-211, https://doi.org/10.1016/j.envpol.2014.06.003, 2014.

Kalafut-Pettibone, A. J., Wang, J., Eichinger, W. E., Clarke, A., Vay, S. A., Blake, D. R., and Stanier, C. O.: Size-resolved aerosol emission factors and new particle formation/growth activity occurring in Mexico City during the MILAGRO 2006 Campaign, Atmos. Chem. Phys., 11, 8861–8881, https://doi.org/10.5194/acp-11-8861-2011, 2011.

Kanawade, V.P., Srivastava, A.K., Ram, K., Asmi, E., Vakkari, V., Soni, V.K., Varaprasad, V. and Sarangi, C.: What caused severe air pollution episode of November 2016 in New Delhi?, Atmos. Environ., 222, 117125, https://doi.org/10.1016/j.atmosenv.2019.117125, 2020.

Kontses, A., Triantafyllopoulos, G., Ntziachristos, L. and Samaras, Z.: Particle number (PN) emissions from gasoline, diesel, LPG, CNG and hybrid-electric light-duty vehicles under real-world driving conditions, Atmos. Environ., 222, 117126, https://doi.org/10.1016/j.atmosenv.2019.117126, 2020.

Kuang, C., Chen, M., Zhao, J., Smith, J., McMurry, P. H., and Wang, J.: Size and time-resolved growth rate measurements of 1 to 5 nm freshly formed atmospheric nuclei, Atmos. Chem. Phys., 12, 3573–3589, https://doi.org/10.5194/acp-12-3573-2012, 2012.

Kulmala, M., Dada, L., Daellenbach, K.r., Yan, C., Stolzenburg, D., Kontkanen, J., Ezhova, E., Hakala, S., Tuovinen, S., Kokkonen, T.V., Kurpp, M., Cai, R., Zhou, Y., Yin, R., Baalbaki, R., Chan, T., Chu, B., Deng, C., Fu, Y., Ge, M., He, H., Heikkinen, L., Junninen, H., Liu, Y., Lu, Y., Nie, W., Rusanen, A., Vakkari,V., Wang, Y., Yang, G., Yao, L., Zheng, J., Kujansuu, J., Kangasluoma, J., Petäjä, T., Paasonen, P., Järvi, L., Worsnop, D., Ding, A., Liu, Y., Wang, L., Jiang, J., Bianchi, F. and Kerminen, V.M.: Is reducing new particle formation a plausible solution to mitigate particulate air pollution in Beijing and other Chinese megacities? Faraday Discussion 226, 221, doi.org/10.1039/D0FD00078G, 2021.

Kulmala M., Luoma K., Virkkula A., Petäjä T., Paasonen P., Kerminen V.-M., Nie W., Qi X., Shen Y., Chi X. and Ding A.: On the mode-segregated aerosol particle number concentration load: contributions of primary and secondary particles in Hyytiälä and Nanjing. Boreal, Env. Res., 21, 319–331. 2016.

Kumar, A., Ambade, B., Sankar, T. K., Sethi, S. S. and Kurwadkar, S.: Source identification and health risk assessment of atmospheric PM2.5-bound polycyclic aromatic hydrocarbons in Jamshedpur, India, Sustainable Cities and Society, 52, 101801, https://doi.org/10.1016/j.scs.2019.101801, 2020.

Kumar, P., Gulia, S., Harrison, R. M. and Khare, M.: The influence of odd–even car trial on fine and coarse particles in Delhi, Environmental Pollution, 225, 20-30, https://doi.org/10.1016/j.envpol.2017.03.017, 2017.

Kumar, P., Pirjola, L., Ketzel, M., and Harrison, R. M.: Nanoparticle emissions from 11 non-vehicle exhaust sources – A review, Atmos. Environ., 67, 252–277, https://doi.org/10.1016/j.atmosenv.2012.11.011, 2013.

Iida, K., Stolzenburg, M.R., McMurry, P.H. and Smith, J.N.: Estimating nanoparticle growth rates from size-dependent charged fractions: Analysis of new particle formation events in Mexico City, J. Geophys. Res., 113, D05207, doi.org/10.1029/2007JD009260, 2008

Liu, J., Jiang, J., Zhang, Q., Deng, J., and Hao, J.: A spectrometer for measuring particle size distributions in the range of 3 nm to 10 μm, Front. Environ. Sci. Eng., 10, 63–72, https://doi.org/10.1007/s11783-014-0754-x, 2016.

Magara-Gomez, K.T., Olson, M.R., McGinnis, J.E., Zhang, M. and Schauer, J.J.: Effect of Ambient Temperature and Fuel on Particle Number Emissions on Light-Duty Spark-Ignition Vehicles, Aerosol Air Qual. Res., 14, 1360-1371. https://doi.org/10.4209/aaqr.2013.06.0183, 2014.

Mahato, S., Pal, S. and Ghosh, K. G.: Effect of lockdown amid COVID-19 pandemic on air quality of the megacity Delhi, India, Science of The Total Environment, 730, 139086, https://doi.org/10.1016/j.scitotenv.2020.139086, 2020.

Masiol, M., Vu, T. V., Beddows, D. C. S. and Harrison, R. M.: Source apportionment of wide range particle size spectra and black carbon collected at the airport of Venice (Italy), Atmospheric Environment, 139, 56-74, https://doi.org/10.1016/j.atmosenv.2016.05.018, 2016.

Mönkkönen, P., Koponen, I. K., Lehtinen, K. E. J., Hämeri, K., Uma, R., and Kulmala, M.: Measurements in a highly polluted Asian mega city: observations of aerosol number size distribution, modal parameters and nucleation events, Atmos. Chem. Phys., 5, 57–66, https://doi.org/10.5194/acp-5-57-2005, 2005.

Nagpure, A.S., Ramaswami, A. and Russell, A.: Characterizing the Spatial and Temporal Patterns of Open Burning of Municipal Solid Waste (MSW) in Indian Cities, Environ. Sci. Technol., 49, 21, 12904–12912, https://doi.org/10.1021/acs.est.5b03243, 2015.

Narain, U. and Krupnick, A., The Impact of Delhi's CNG Program on Air Quality. RFF Discussion Paper No. 07-06, Available at SSRN: https://ssrn.com/abstract=969727 or http://dx.doi.org/10.2139/ssrn.969727, 2007.

Ondráček, J., Ždímal, V., Smolík, J., and Lazaridis, M.: A Merging Algorithm for Aerosol Size Distribution from Multiple Instruments, Water Air Soil Pollut., 199, 219–233, https://doi.org/10.1007/s11270-008-9873-y, 2009.

Pant, P. and Harrison, R. M.: Critical Review of Receptor Modelling for Particulate Matter: A Case Study of India, Atmos. Environ., 49, 1-12, https://doi.org/10.1016/j.atmosenv.2011.11.060, 2012.

Pant, P., Baker, S. J., Goel, R., Guttikunda, S., Goel, A., Shukla, A. and Harrison, R.M.: Analysis of size-segregated winter season aerosol data from New Delhi, India, Atmos. Poll. Res., 7, 1, 100-109, https://doi.org/10.1016/j.apr.2015.08.001., 2016.

R Core Team, 2015. R: a Language and Environment for Statistical Computing. R Foundation for Statistical Computing, Vienna, Austria. http://www.R-project.org/.

Rai, P., Furger, M., Haddad, I.E., Kumar, V., Wang, L., Singh, A., Dixit, K., Bhattu, D., Petit, J.E., Ganguly, D., Rastogi, N., Baltensperger, U., Tripathi, S.N., Slowik, J.G. and Prévôt, A.S.H.: Real-time measurement and source apportionment of elements in Delhi's atmosphere, Science of The Total Environment, 742, 140332, https://doi.org/10.1016/j.scitotenv.2020.140332, 2020.

Rodríguez, S. and Cuevas, E.: The contributions of “minimum primary emissions” and “new particle formation enhancements” to the particle number concentration in urban air, Journal of Aerosol Science 38, 1207-1219, https://doi.org/10.1016/j.jaerosci.2007.09.001, 2007.

Rodríguez-Urrego, D. and Rodríguez-Urrego, L.: Air quality during the COVID-19: PM2.5 analysis in the 50 most polluted capital cities in the world, Environmental Pollution, 266, 1, 115042, https://doi.org/10.1016/j.envpol.2020.115042, 2020.

Salvador, P., Barreiro, M., Gómez-Moreno, F. J., Alonso-Blanco, E. and Artíñano, B.: Synoptic classification of meteorological patterns and their impact on air pollution episodes and new particle formation processes in a south European air basin, Atmos.c Environ., 245, 118016, https://doi.org/10.1016/j.atmosenv.2020.118016, 2021.

912 Sarangi, B., Aggarwal, S. G., and Gupta, P. K.: A simplified approach to calculate particle growth
913 rate due to self-coagulation, scavenging and condensation using SMPS measurements during a
914 particle growth event in New Delhi, Aerosol and air quality research, 15(1), 166-179, https://doi:
915 10.4209/aaqr.2013.12.0350, 2015.
916
917 Sarangi, B., Aggarwal, S. G., Kunwar, B., Kumar, S., Kaur, R., Sinha, D., Tiwari, S. and
918 Kawamura, K.: Nighttime particle growth observed during spring in New Delhi: Evidences for the
919 aqueous phase oxidation of SO2, Atmospheric environment, 188, 82-96,
920 https://doi.org/10.1016/j.atmosenv.2018.06.018, 2018
921
922 Schmid, O., Karg, E., Hagen, D. E., Whitefield, P. D. and Ferron, G. A.: On the Effective Density
923 of Non-Spherical Particles as Derived From Combined Measurements of Aerodynamic and
924 Mobility Equivalent Size, Atmos. Environ., 38, 431–443.
925 https://doi.org/10.1016/j.jaerosci.2007.01.002, 2007.
926
927 Schreiber, D., Forss, A. M., Mohr, M. and Dimopoulos, P.: Particle Characterisation of Modern
928 CNG, Gasoline and Diesel Passenger Cars, 8th International Conference on Engines for
929 Automobiles, Technical Paper 2007-24-0123, ISSN: 0148-7191, e-ISSN: 2688-3627,
930 https://doi.org/10.4271/2007-24-0123, 2007.
931
932 Tiwari, S., Bisht, D.S., Srivastava, A.K., Pipal, A.S., Taneja, A., Srivastava, M.K. and Attri, S.D.:
933 Variability in atmospheric particulates and meteorological effects on their mass concentrations over
934 Delhi, India, Atmospheric Research, 145–146, 45-56,
935 https://doi.org/10.1016/j.atmosres.2014.03.027, 2014.
936
937 Thamban, N.M., Lalchandani, V., Kumar, V., Mishra, S., Bhattu, D., Slowik, J.G., Prevot, A.S.H.,
938 Satish, R., Rastogi, N., Tripathi, S.N.: Evolution of size and composition of fine particulate matter
939 in the Delhi megacity during later winter, Atmospheric Environment, 267,118752,
940 doi.org/10.1016/j.atmosenv.2021.118752. 2021.
941
942 Toumasatos, Z., Kontses, A., Doulgeris, S., Samaras, Z. and Ntziachristos, L.: Particle emissions
943 measurements on CNG vehicles focusing on Sub-23nm, Aerosol Science and Technology, 55,
944 2, 182-193, https://doi.org/10.1080/02786826.2020.1830942, 2021.
945
946 Tyagi, S., Tiwari, S., Mishra, A., Hopke, P.K., Attri, S.D., Srivastava, A.K. and Bisht, D. S.: Spatial
947 variability of concentrations of gaseous pollutants across the National Capital Region of Delhi,
948 India, Atmospheric Pollution Research, 7, 5, 808-816, https://doi.org/10.1016/j.apr.2016.04.008,
949 2016.
950
951 Vu, T. V., Delgado-Saborit, J. M. and Harrison, R. M.: Particle number size distributions from
952 seven major sources and implications for source apportionment studies. Atmospheric Environment,
953 122, 114-132, https://doi.org/10.1016/j.atmosenv.2015.09.027, 2015.
954 Wu, T. and Boor, B. E.: Urban aerosol size distributions: a global perspective, Atmos. Chem. Phys.,
955 21, 8883–8914, https://doi.org/10.5194/acp-21-8883-2021, 2021.
956
957 Yadav, R., Sahu, L.K., Beig, G. and Jaaffrey, S.N.A.: Role of long-range transport and local
958 meteorology in seasonal variation of surface ozone and its precursors at an urban site in India,
959 Atmospheric Research, 176–177, 96-107,https://doi.org/10.1016/j.atmosres.2016.02.018, 2016.
960
961 Zhang, Y. M., Zhang, X. Y., Sun, J. Y., Lin, W. L., Gong, S. L., Shen, X. J. and Yang, S.:
962 Characterization of new particle and secondary aerosol formation during summertime in Beijing,

963 China, Tellus B: Chemical and Physical Meteorology, 63:3, 382-394,
964 https://doi.org/10.1111/j.1600-0889.2011.00533.x, 2011.
965
966 Zhu, C., Li, J.G., Wang, L., Morawska, L., Zhang, X. and Zhang, Y.L.: Size-resolved particle
967 distribution and gaseous concentrations by real-world road tunnel measurement, Indoor and Built
968 Environment, 23, 2, 225-235, https://doi.org/10.1177/1420326X13509290, 2014.

FIGURE CAPTIONS:

Figure 1. Comparison of average particle number counts (#/cm^3) for nucleation, aitken, accumulation, large fine and coarse modes of PM between 15 nm and 10 µm in all seasons, and the volume contributions for comparison.

Figure 2. Average diurnal variation of particle number counts for nucleation, Aitken, accumulation, large fine and coarse modes and $PM_{2.5}$, BC, NO and NO_2 in autumn, summer and winter.

Figure 3. Average diurnal variation of total particle number counts (between 15 and 10 µm) for weekday average (Monday to Friday), Saturday and Sunday in Delhi. (Summer data are very limited. There are no data on Friday afternoon, night and Saturday early morning (Figure S6)).

Figure 4. Diurnal contour plots for particles derived by SMPS between 15 and 660 nm averaged for each season (a: winter, b: Autumn and c: Summer) and for 3 June 2018 data when a NPF event probably occurred (d), the solid line showing the NO_x mixing ratio. ~~Note the different scales for the seasons presented.~~

Figure 5. The hourly average of day and night particle numbers for all modes from the wide range particle sizes derived from the merged data. UFP = Nucleation +Aitken, PN_1 = UFP+Accumulation, PN_{10} = PN_1+Large Fine+Coarse.

Figure 6. Seasonal average (line) and standard deviation (shadow) of particle number size distributions.

Figure 7. Hourly average day and night (left side) and during day hours (right side) particle number distributions in autumn, summer and winter in Delhi.

Figure 8. Diurnal change of the geometric mean diameter (GMD) calculated for winter, autumn and summer seasons. Growth rates (nm/hour) are calculated from dGMD/dt.

Figure 9. Hourly average particle number, volume and area distributions in the winter (a), autumn (b) and summer (c) in Delhi.

Figure 10. Correlation coefficient (R) between the hourly average PNs of five particle size fractions (left side) and NO, NO_2, BC (right side).

Figure 11. Polar plots of PNs (#/cm^3) for five particle size fractions in winter, autumn and summer in Delhi.

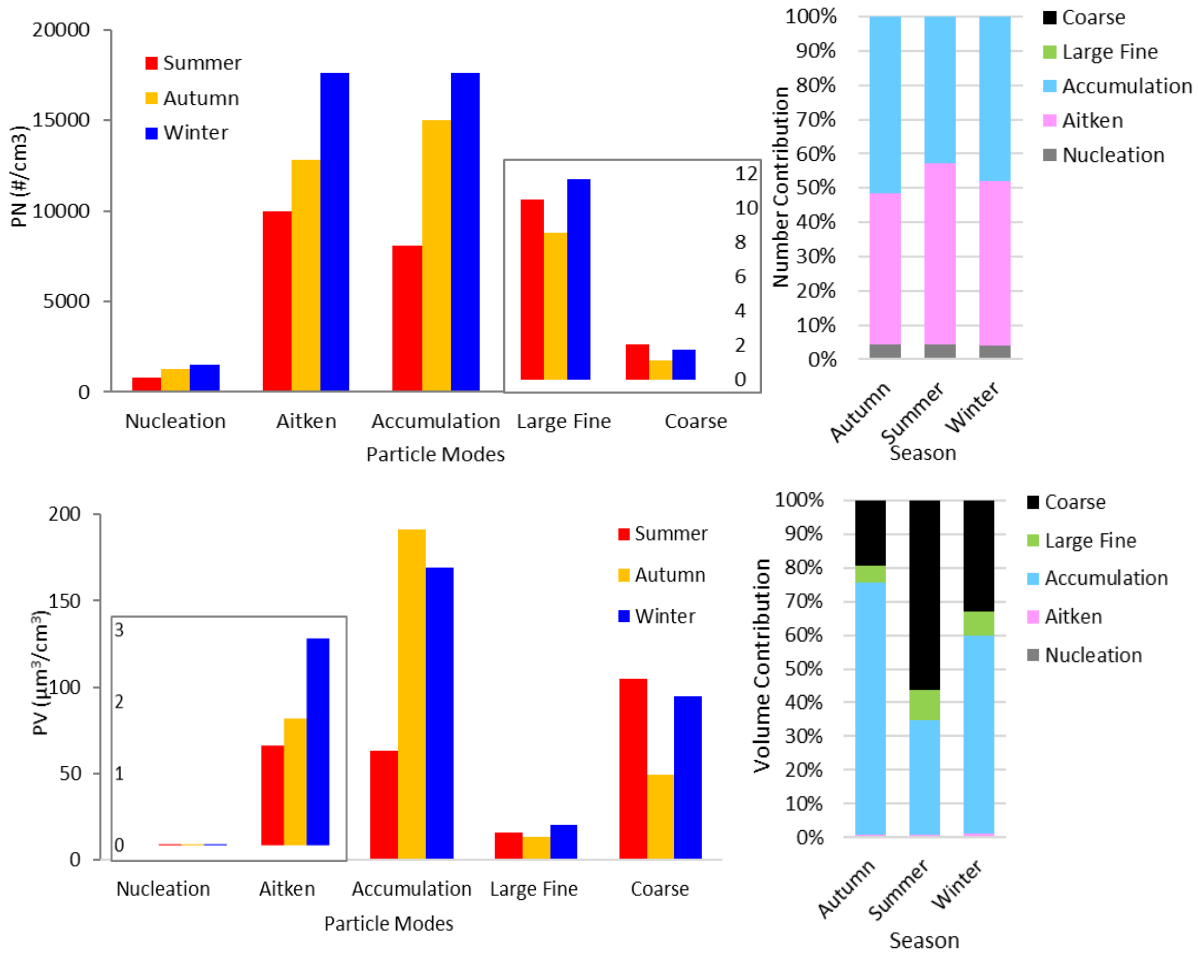

Figure 1. Comparison of average particle number counts (#/cm^3) for nucleation, aitken, accumulation, large fine and coarse modes of PM between 15 nm and 10 µm in all seasons, and the volume contributions for comparison.

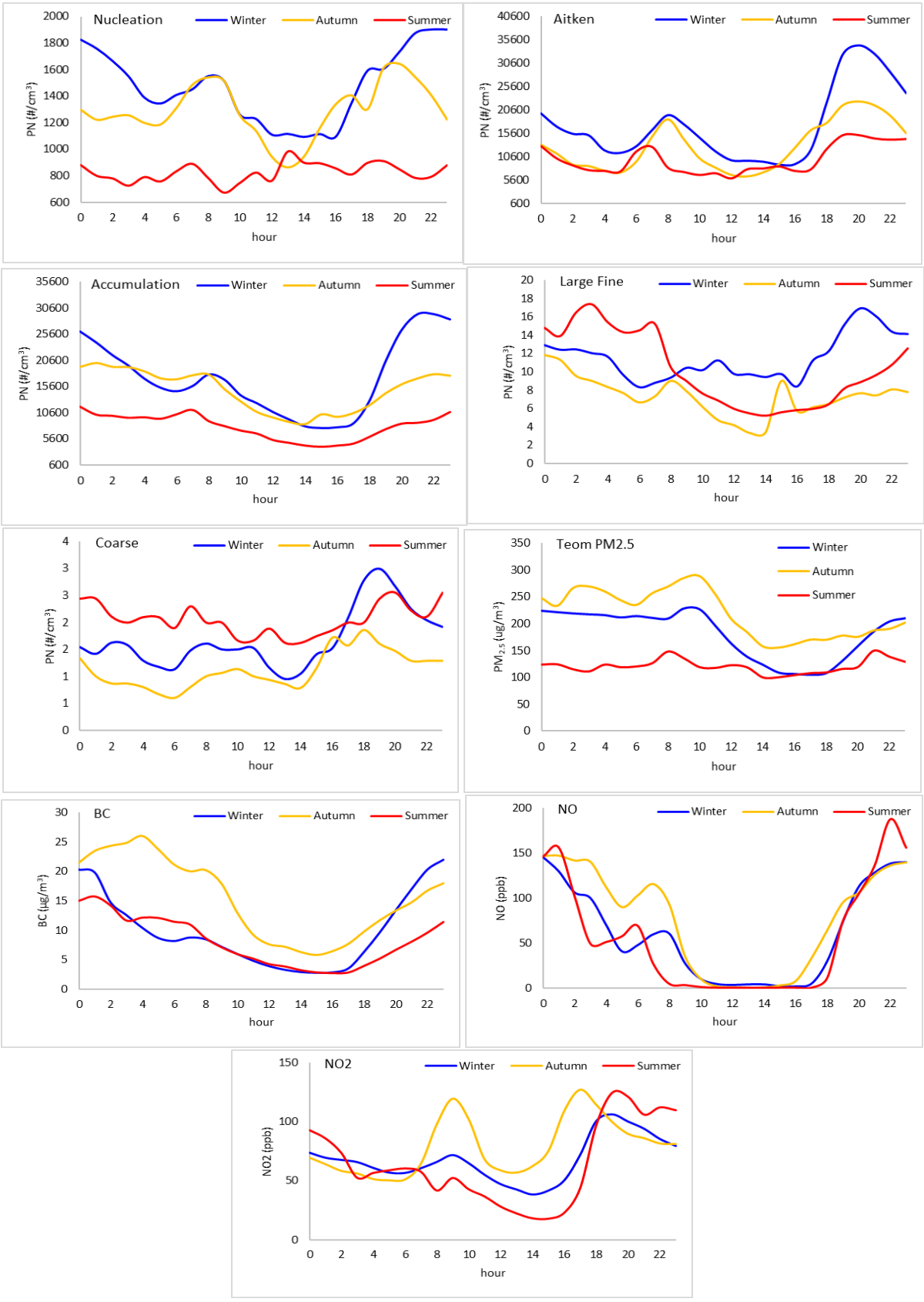

Figure 2. Average diurnal variation of particle number counts for nucleation, Aitken, accumulation, large fine and coarse modes and $PM_{2.5}$, BC, NO and NO_2 in autumn, summer and winter.

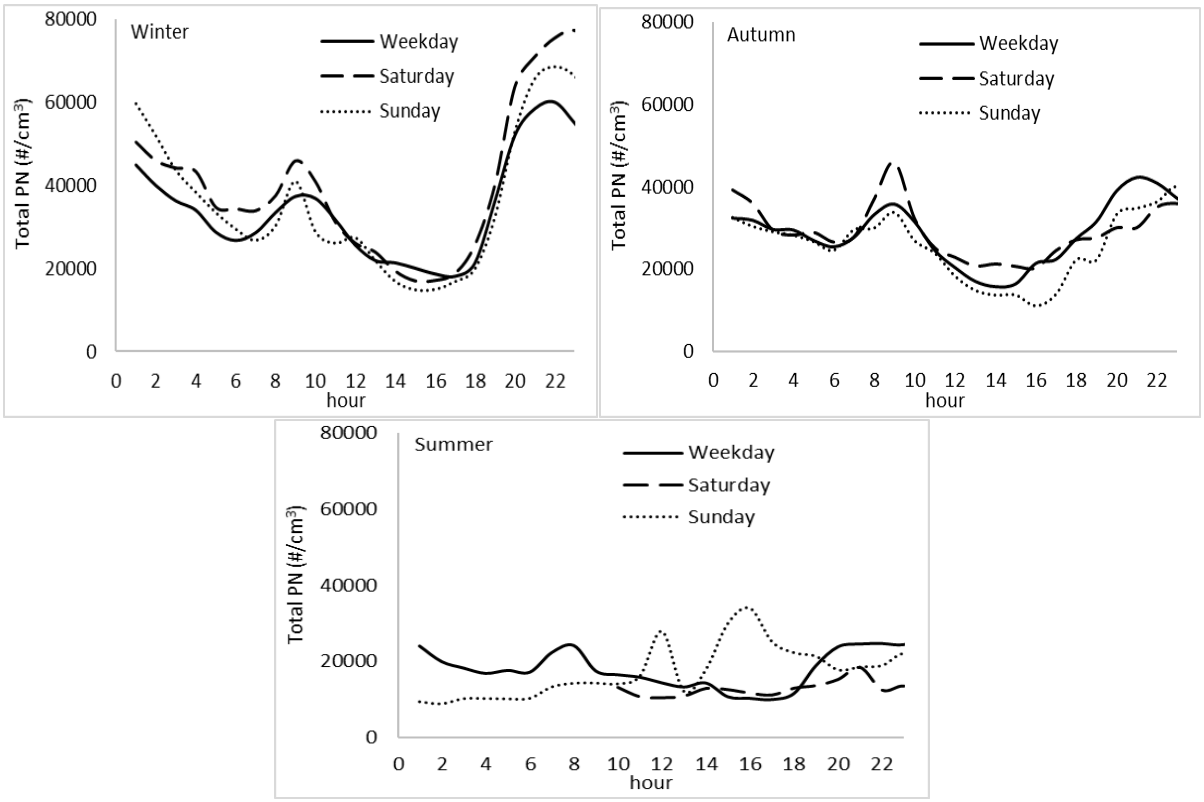

Figure 3. Average diurnal variation of total particle number counts (between 15 and 10 µm) for weekday average (Monday to Friday), Saturday and Sunday in Delhi. (Summer data are very limited. There are no data on Friday afternoon, night and Saturday early morning (Figure S6)).

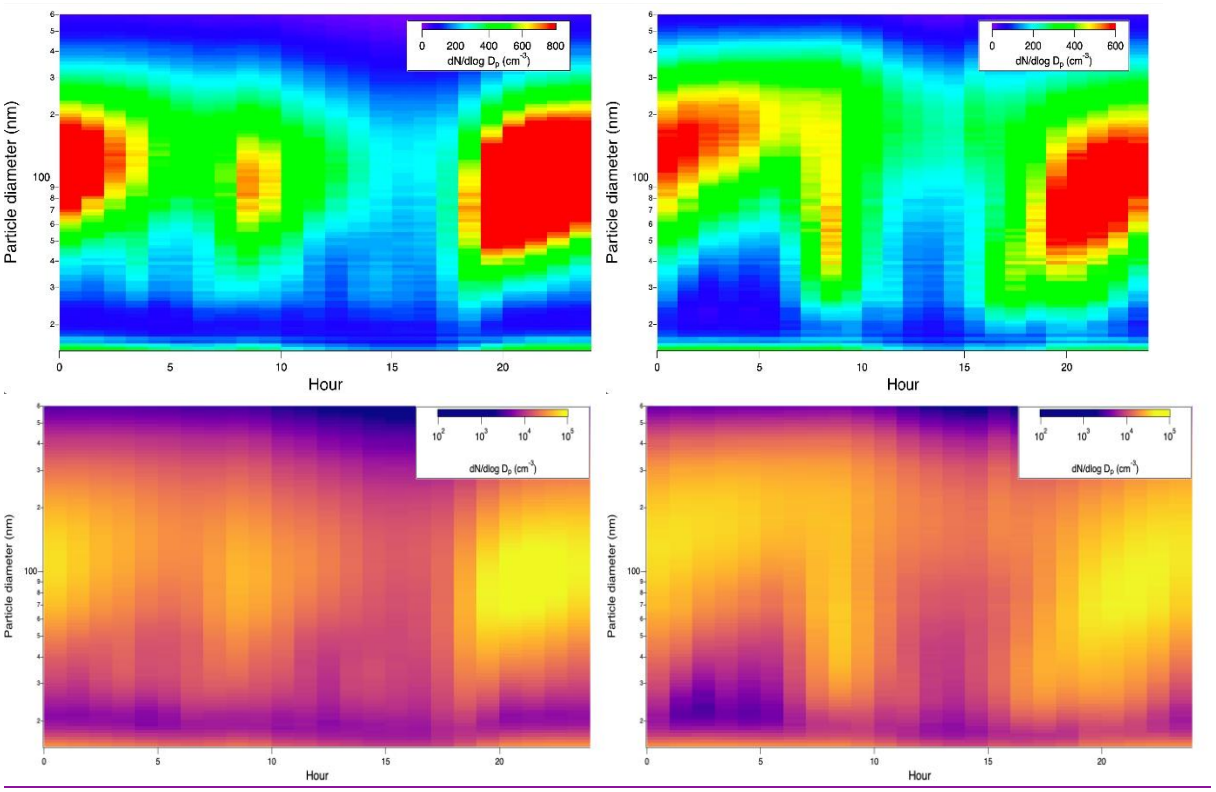

a) Winter b) Autumn

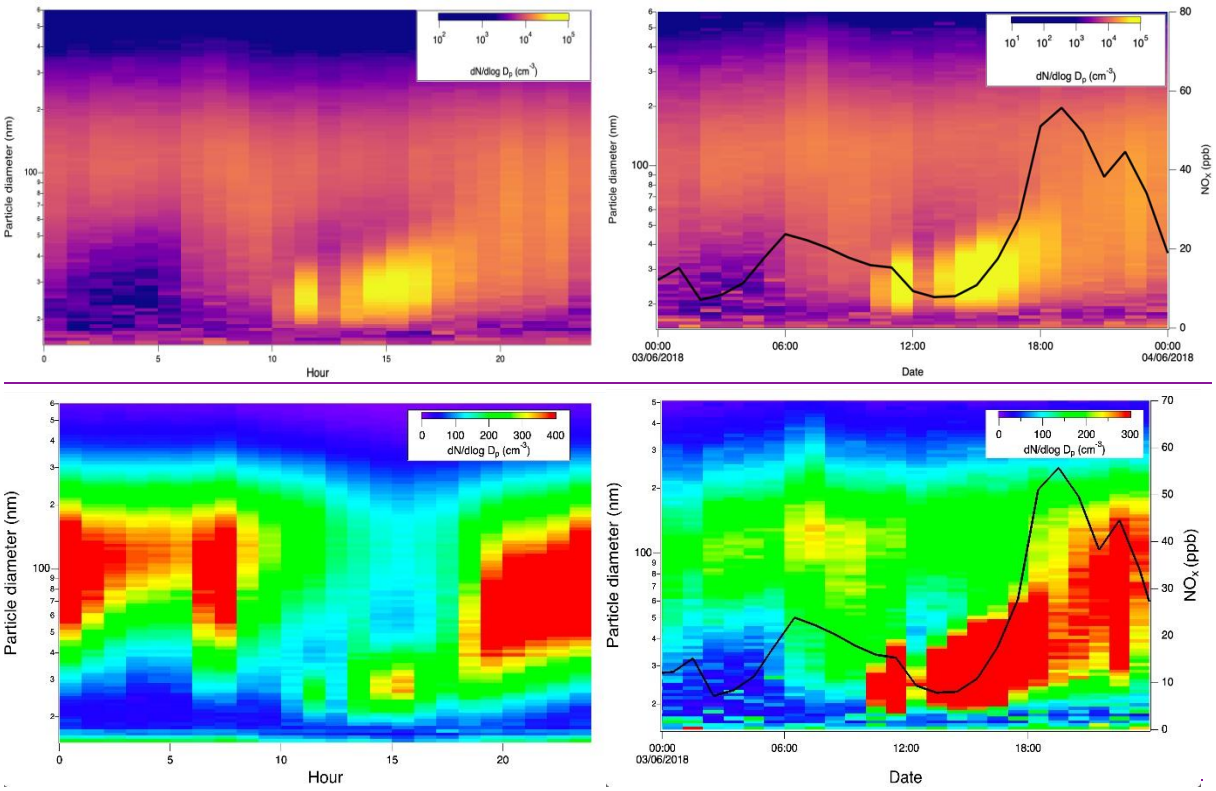

c) Summer d) 3 June 2018

Figure 4. Diurnal contour plots for particles derived by SMPS between 15 and 660 nm averaged for each season (a: winter, b: Autumn and c: Summer) and for 3 June 2018 data when a NPF event

probably occurred (d), the solid line showing the NO_x mixing ratio. ~~Note the different scales for the seasons presented.~~

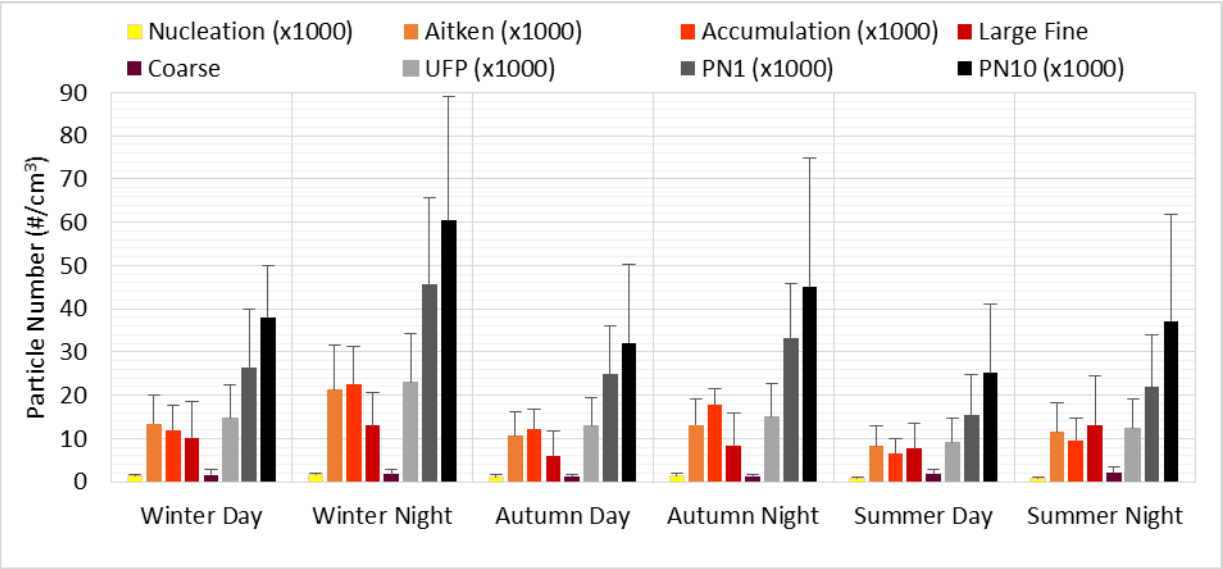

Figure 5. The hourly average of day and night particle numbers for all modes from the wide range particle sizes derived from the merged data. UFP = Nucleation +Aitken, PN_1 = UFP+Accumulation, PN_{10} = PN_1+Large Fine+Coarse.

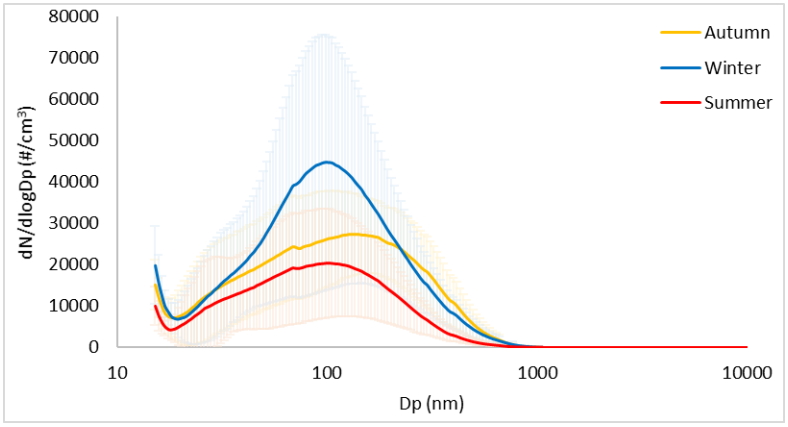

1055

1056 **Figure 6.** Seasonal average (line) and standard deviation (shadow) of particle number size
1057 distributions.
1058

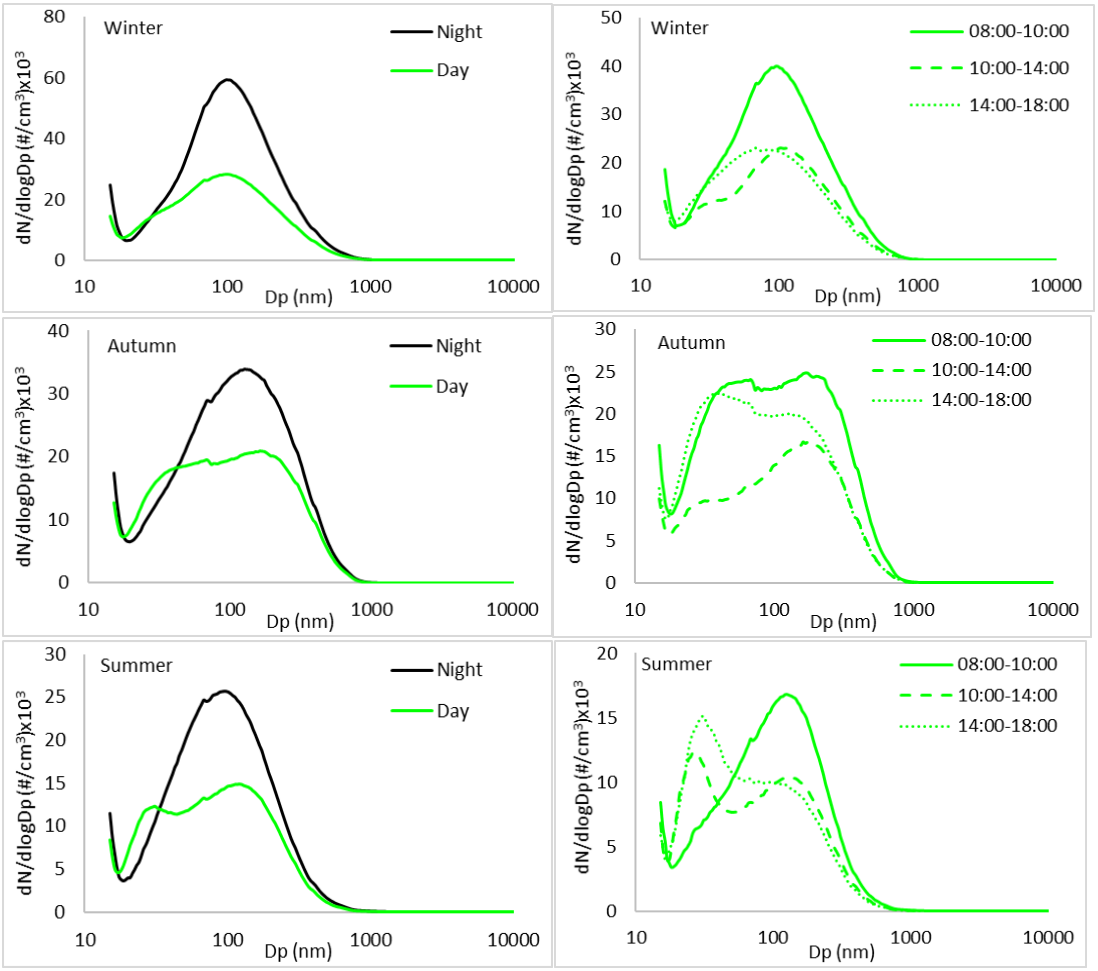

Figure 7. Hourly average day and night (left side) and during day hours (right side) particle number distributions in autumn, summer and winter in Delhi.

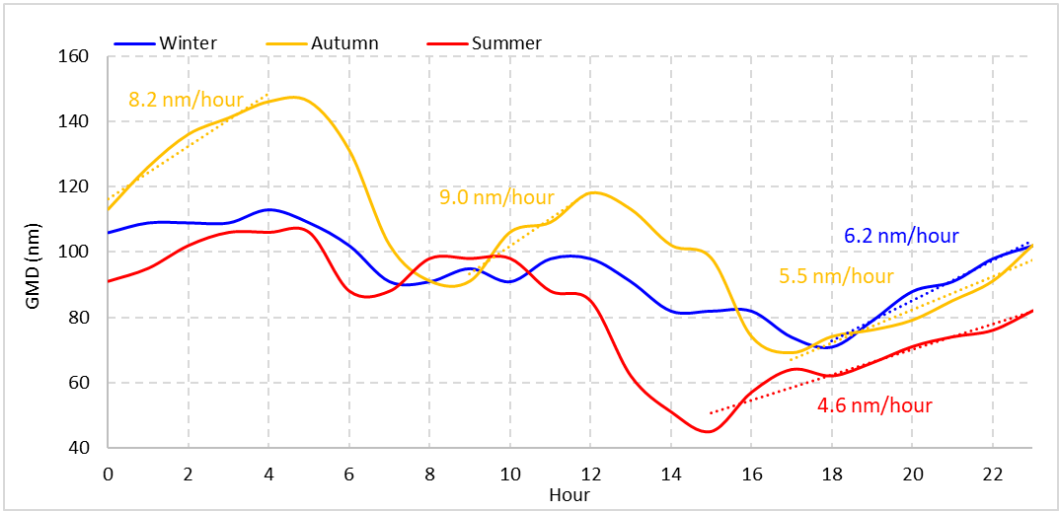

Figure 8. Diurnal change of the geometric mean diameter (GMD) calculated for winter, autumn and summer seasons. Growth rates (nm/hour) are calculated from dGMD/dt.

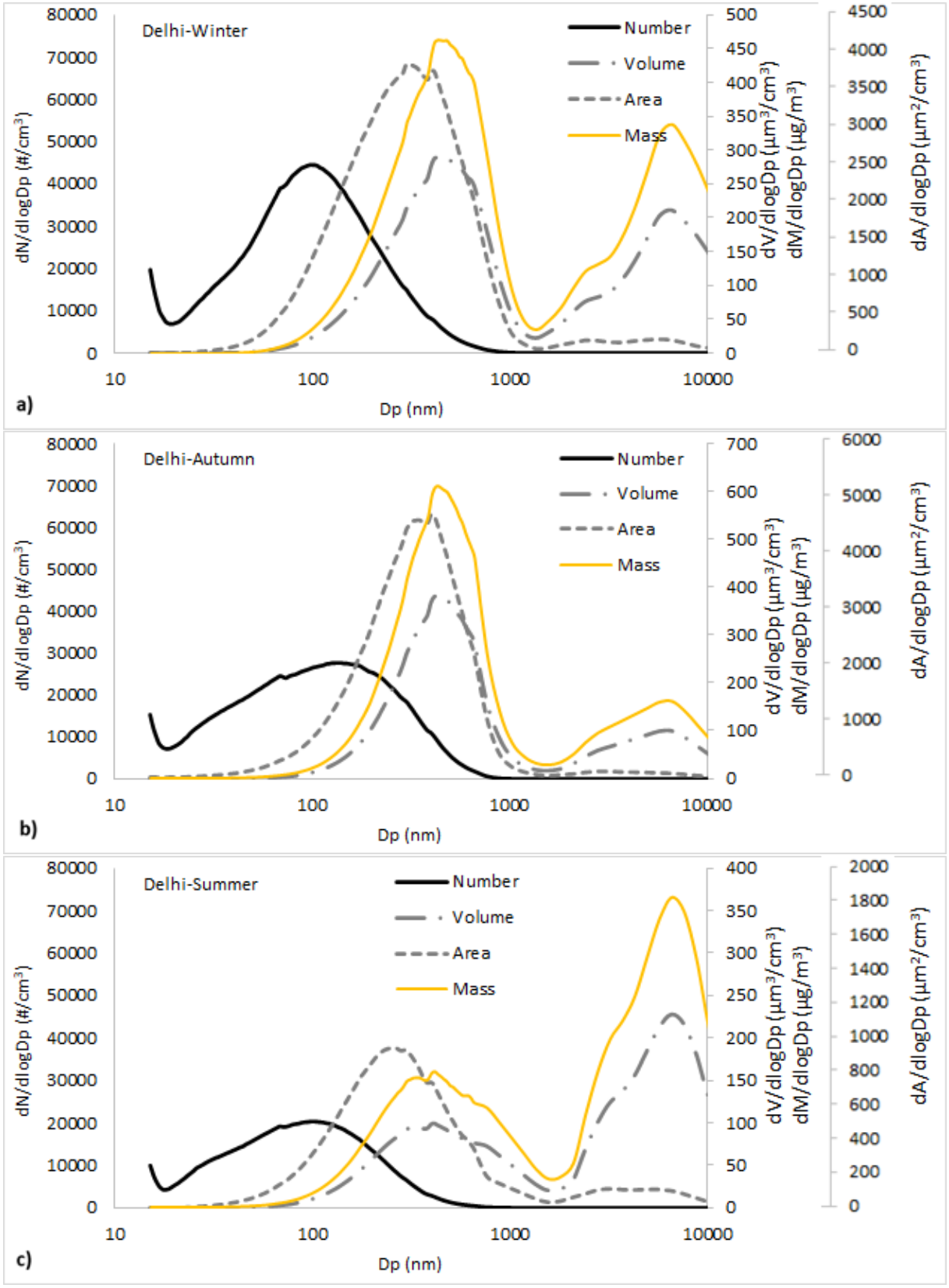

Figure 9. Hourly average particle number, volume and area distributions in the winter (a), autumn (b) and summer (c) in Delhi.

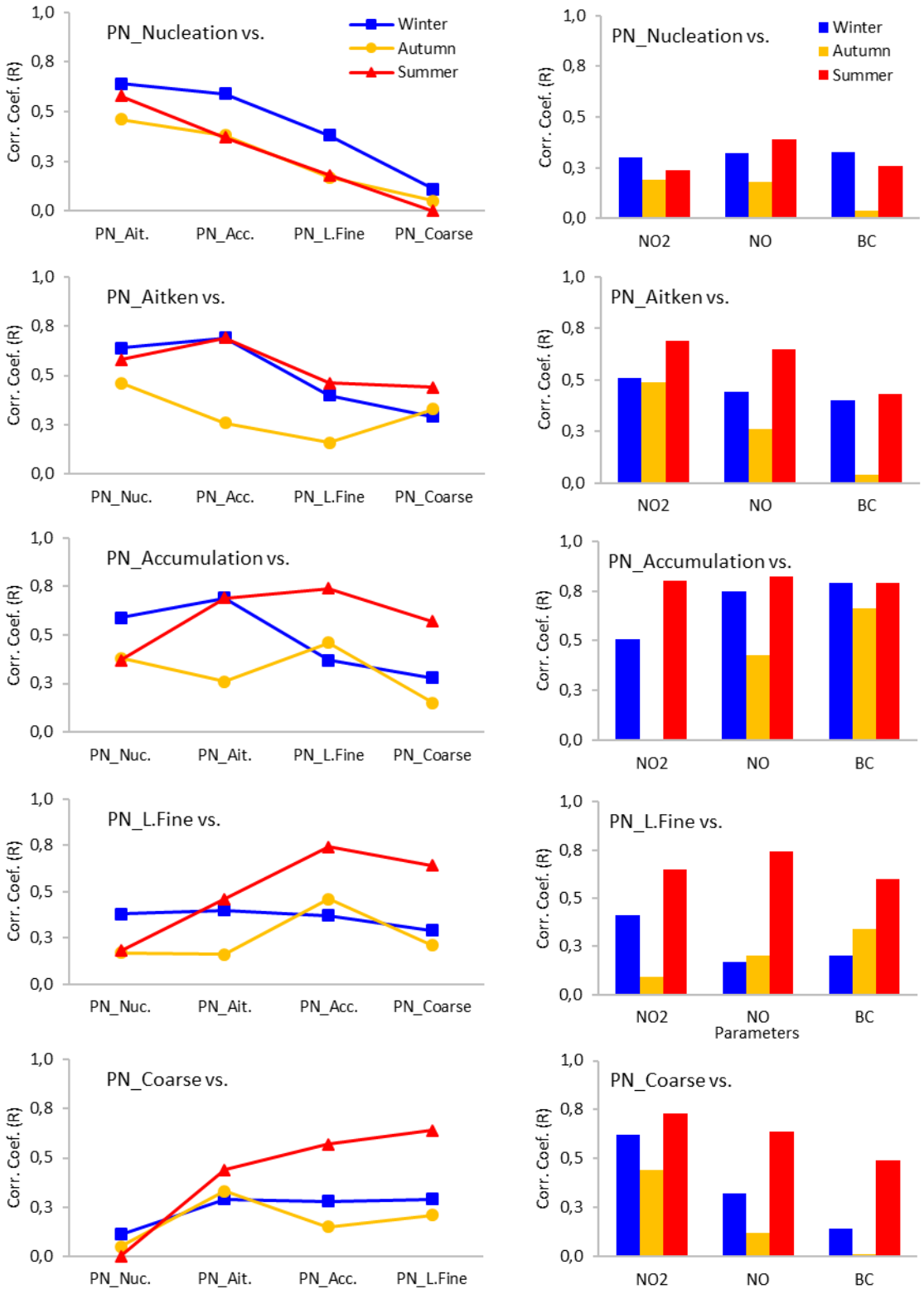

Figure 10. Correlation coefficient (R) between the hourly average PNs of five particle size fractions (left side) and NO, NO_2, BC (right side).

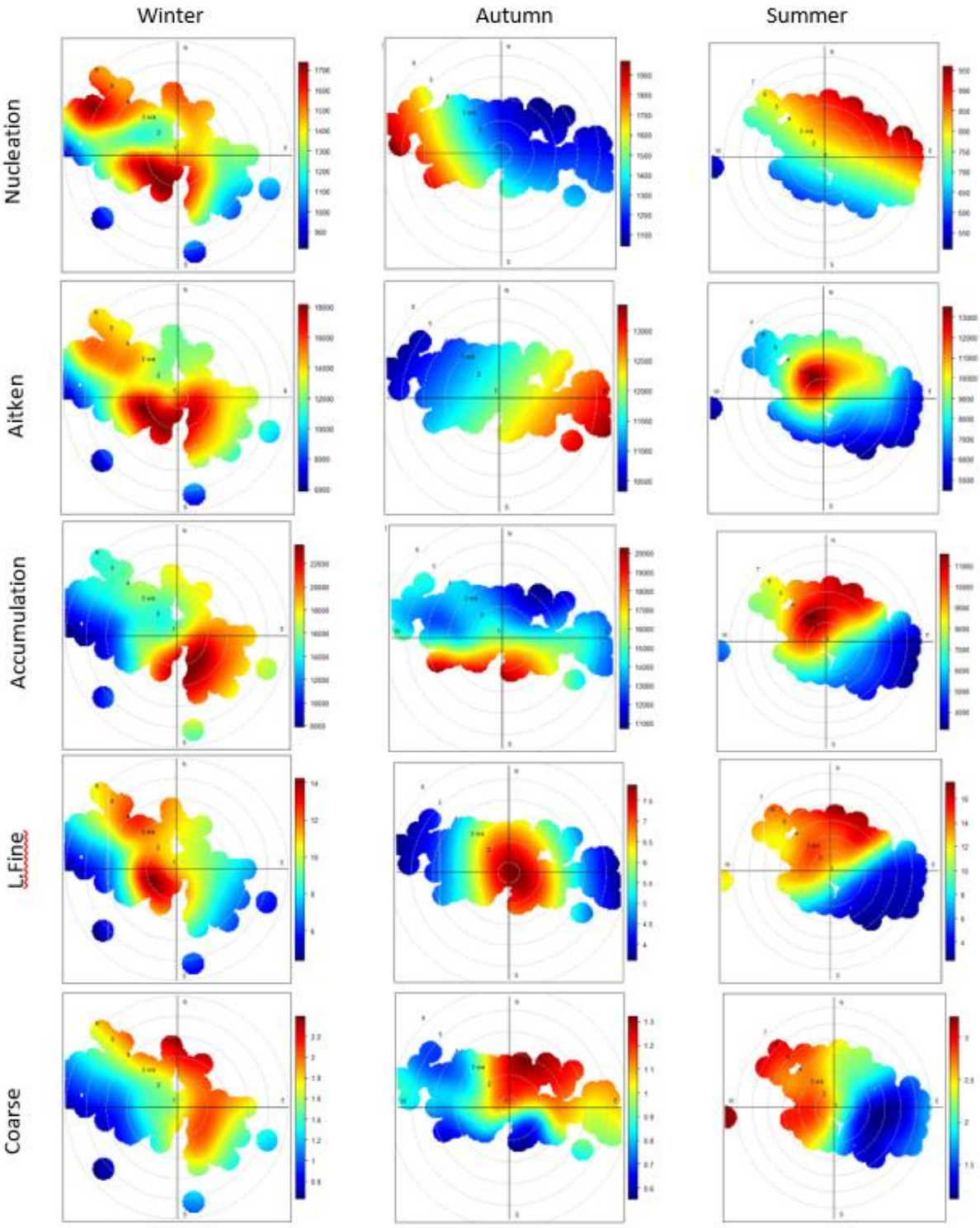
Winter
Autumn
Summer
Nucleation
Aitken
Accumulation
L.Fine
Coarse

1084

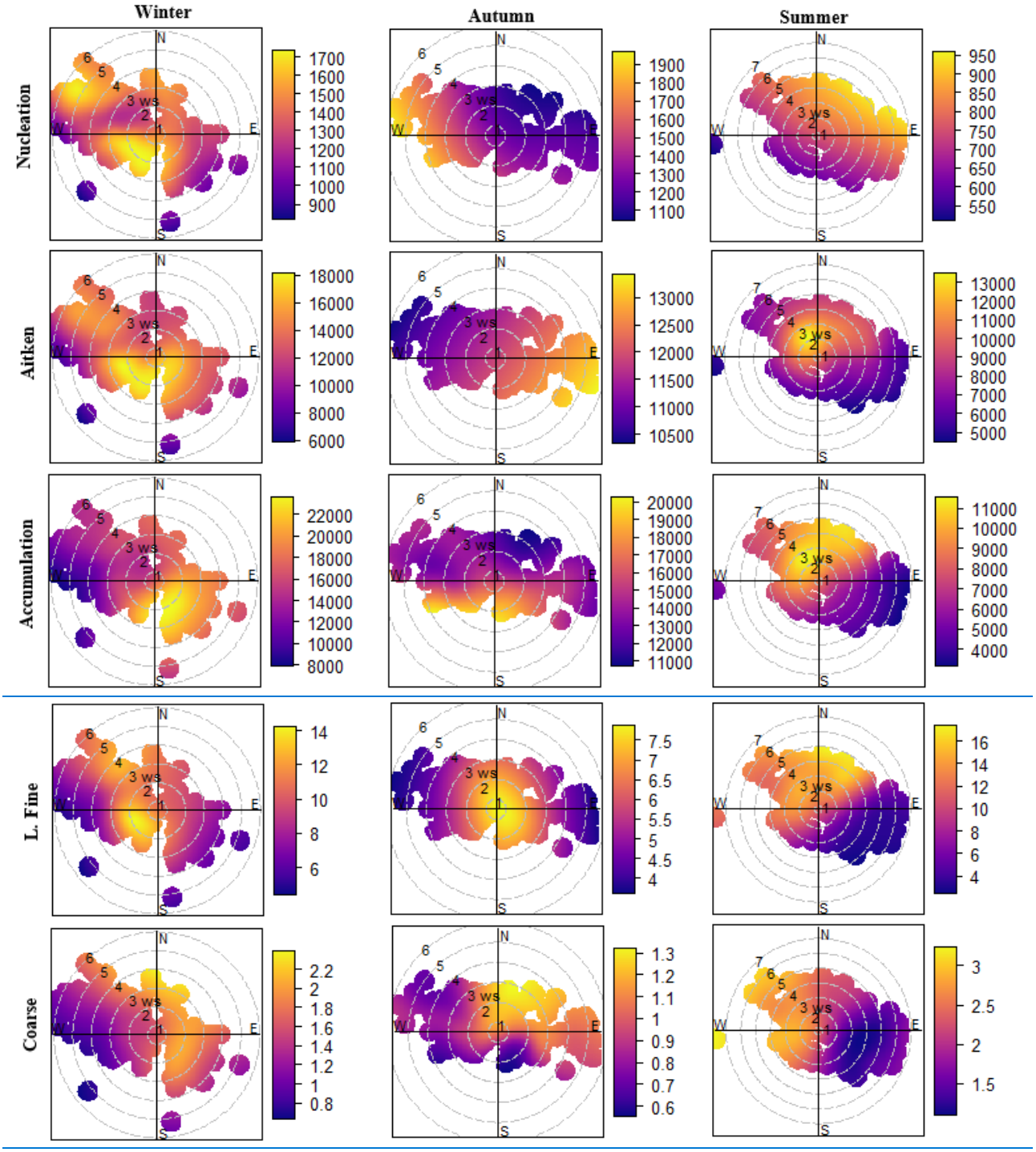

Figure 11. Polar plots of PNs (#/cm^3) for five particle size fractions in winter, autumn and summer in Delhi.

SUPPLEMENTARY INFORMATION

Measurement Report: Interpretation of Wide Range Particulate Matter Size Distributions in Delhi

Ülkü Alver Şahin, Roy M Harrison, Mohammed S. Alam, David C.S. Beddows, Dimitrios Bousiotis, Zongbo Shi, Leigh R. Crilley, William Bloss, James Brean, Isha Khanna and Rulan Verma

Figure S1: IIT Sampling Location in Delhi.

Table S1: Merged Data Grade and Set limits . [O: Is there an overlap? N: Is the data scattered over the overlap? F: Fraction of points which match, S: Smoothness of overlap across the SMPS and GRIMM data.]

Criterion				Point
O: 1: Yes; 0: No.	N: 3 – None; 2- either SMPS or GRIMM; 1 – over both SMPS and GRIMM.	F: 3 – All; 2- most; 1- None	S: 3 – smooth; 2- bumpy; 1- Stepped.	(9/27) x O x N x F x S 9 is perfect, 0 and 1 are unacceptable and are excluded from data set.
1	3	3	3	9 (PERFECT)
1	3	3	2	6 (KEEP)
1	3	2	3	6 (KEEP)
1	2	3	3	6 (KEEP)
1	3	1	2	6 (ACCEPTABLE)
1	3	1	3	6 (ACCEPTABLE)
1	2	1	3	6 (ACCEPTABLE)
1	1	2	3	2 (IMPROVE)
1	1	3	2	2 (IMPROVE)
1	3	2	1	2 (IMPROVE)
1	1	1	3	1 (REJECT)
1	1	3	1	1 (REJECT)
1	3	1	1	1(REJECT)
0	3	3	3	0 (REJECT)

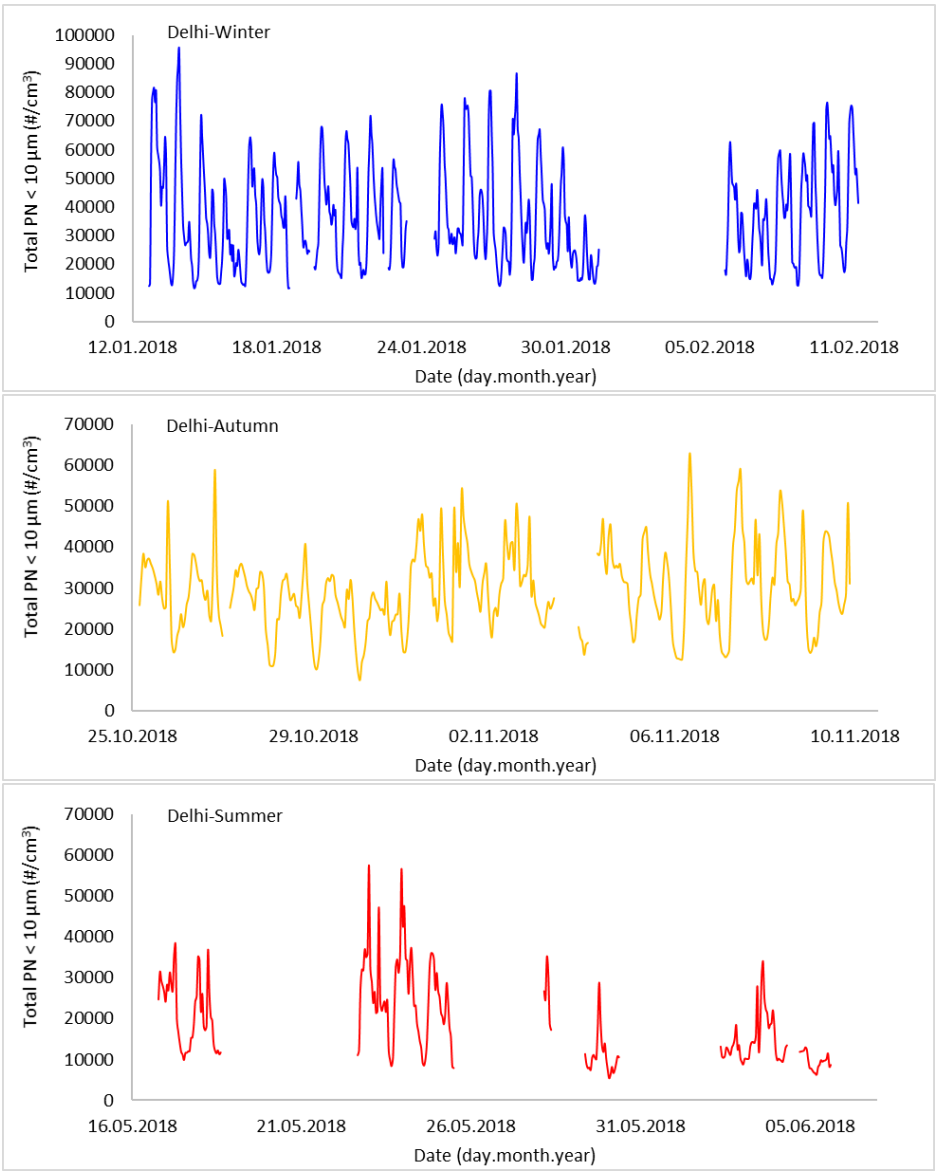

Figure S2: Time series of particle number counts for the sum of nucleation, Aitken, accumulation, fine and coarse modes of PM from the SMPS and Grimm instruments for all season in Delhi.

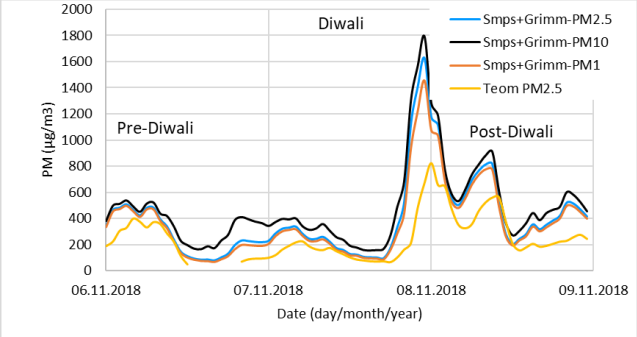

Figure S3: Particle concentration change during Diwali in 2018 in Delhi.

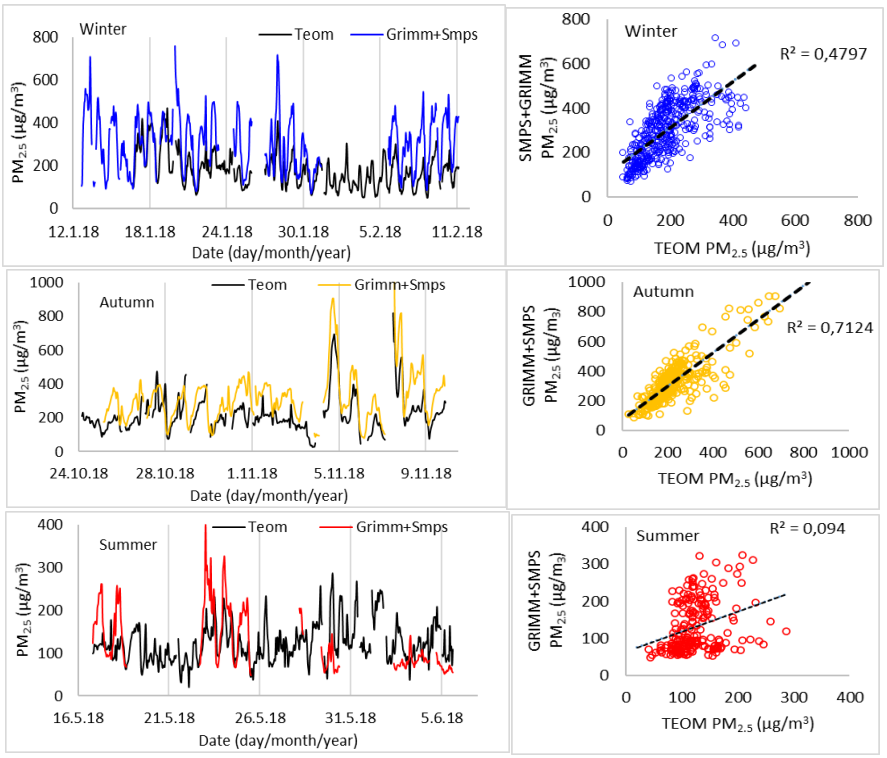

Figure S4: Comparison of $PM_{2.5}$ measured by SMPS+GRIMM and TEOM in Delhi for three seasons.

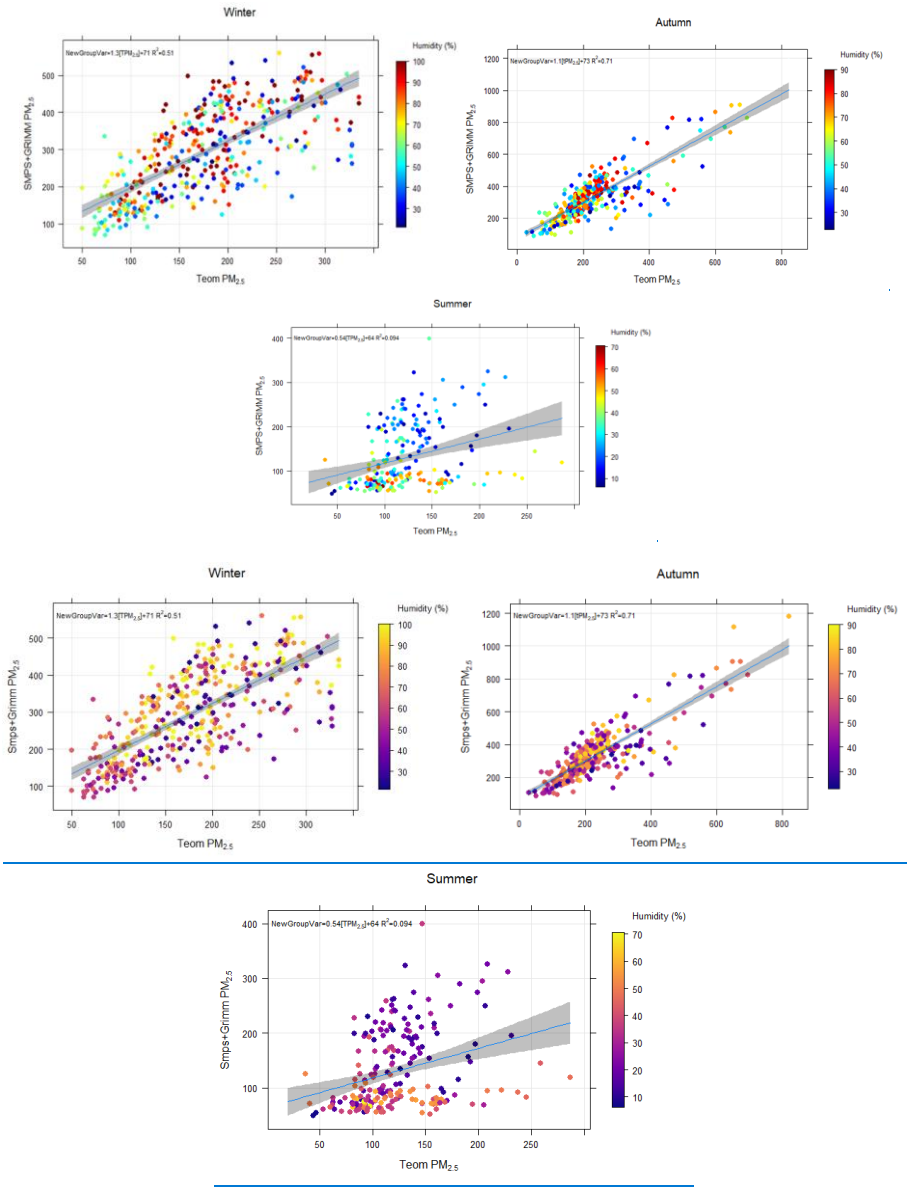

Figure S5: Comparison of $PM_{2.5}$ measured by SMPS+GRIMM and TEOM with relative humidity in Delhi for three seasons.

Table S2: Descriptive statistics of particle number counts (#/cm^3) calculated using every 1 hour measurements for nucleation, Aitken, accumulation, large fine and coarse modes of PN between 15 nm and 10 µm derived by SMPS and Grimm in all seasons.

Seasons	PN modes	**Descriptive Statistics**			
		Range (Min-Max)	Mean	Median	Std. Deviation
Autumn	Nucleation	338-5033	1296	1147	617
	Aitken	2406-44009	12828	11416	6429
	Accumulation	4620-46655	15186	15191	5677
	Large Fine	1-126	9	6	13
	Coarse	0-5	1	1	1
	Total	7507-62756	29355	28528	9883
Summer	Nucleation	302-2504	821	780	310
	Aitken	2237-32521	9965	7963	6084
	Accumulation	2871-27211	8107	5899	4736
	Large Fine	1-5821186	11	6	9
	Coarse	0-5	2	2	1
	Total	5436-57565	18906	15362	10121
Winter	Nucleation	510-3159	1489	1430	541
	Aitken	3356-51293	17610	15571	9682
	Accumulation	3901-50466	17599	15221	9276
	Large Fine	3-6021976	12	10	8
	Coarse	0-9	2	1	1
	Total	11506-95068	36730	33053	17815

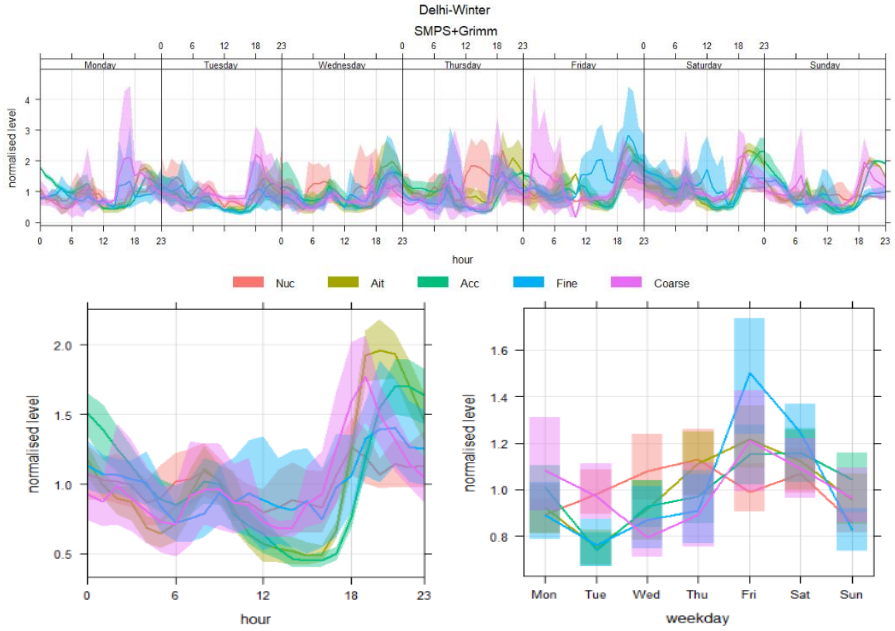
Delhi-Winter
SMPS+Grimm
Monday
Tuesday
Wednesday
Thursday
Friday
Saturday
Sunday
normalised level
hour
Nuc
Ait
Acc
Fine
Coarse
normalised level
hour
normalised level
Mon
Tue
Wed
Thu
Fri
Sat
Sun
weekday

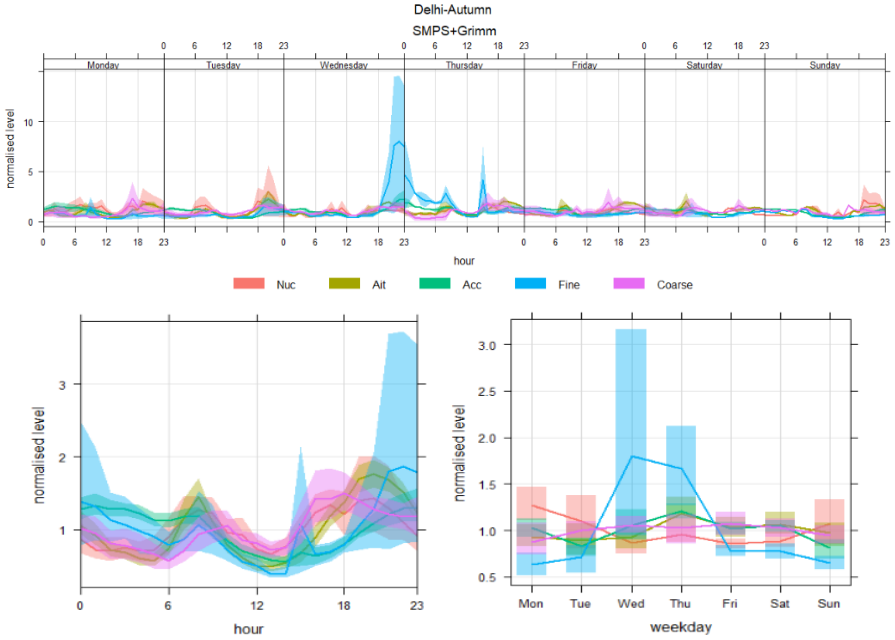
Delhi-Autumn
SMPS+Grimm
Monday
Tuesday
Wednesday
Thursday
Friday
Saturday
Sunday
normalised level
hour
Nuc
Ait
Acc
Fine
Coarse
normalised level
hour
normalised level
Mon
Tue
Wed
Thu
Fri
Sat
Sun
weekday

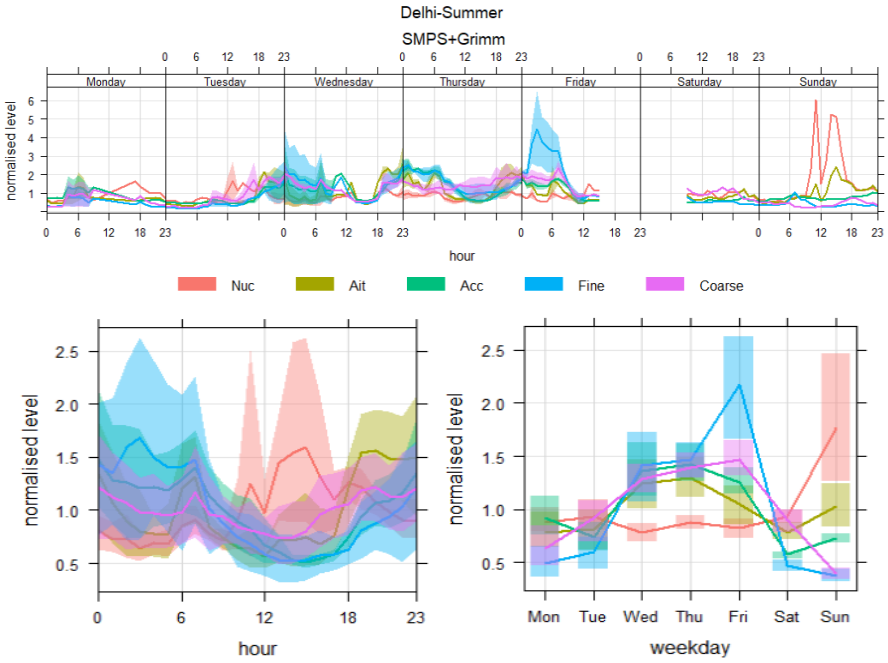

Figure S6: Normalized time variation of all particle fractions (Nuc: Nucleation <25 nm, Ait: Aitken 25-100 nm, Acc: Accumulation 100-1000 nm, Fine: 1-2.5 µm, Coarse: 2.5-10 µm number counts (between 15.1 nm and 10 µm) derived from the SMPS and Grimm instruments for winter, autumn and summer in Delhi.

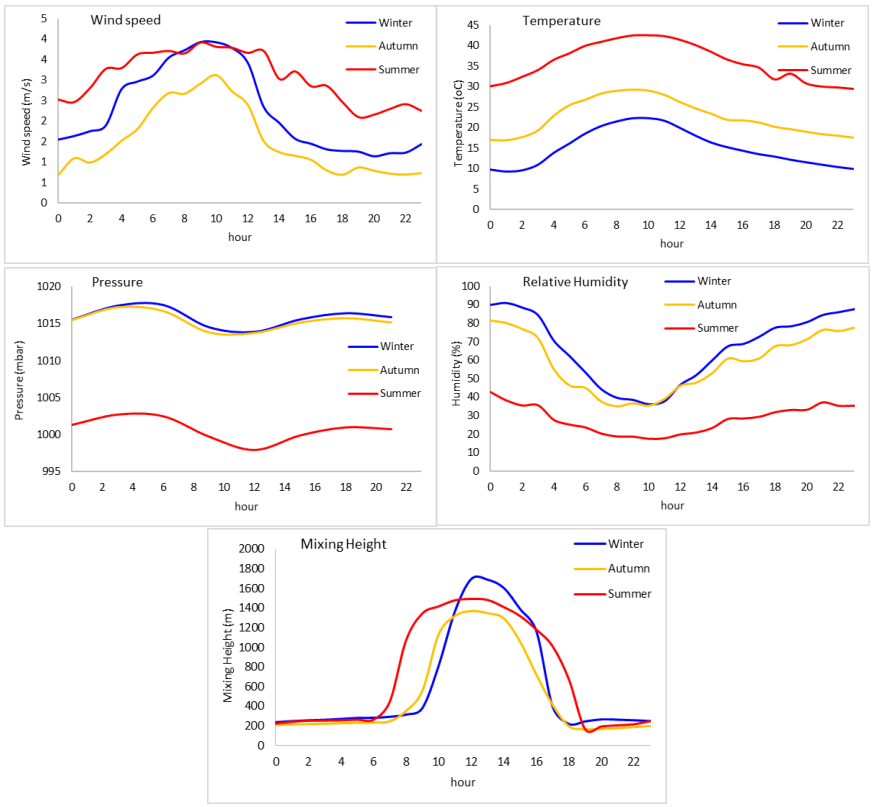

Figure S7: Average diurnal variation of meteorological parameters during the PN measurement campaign in autumn, summer and winter.

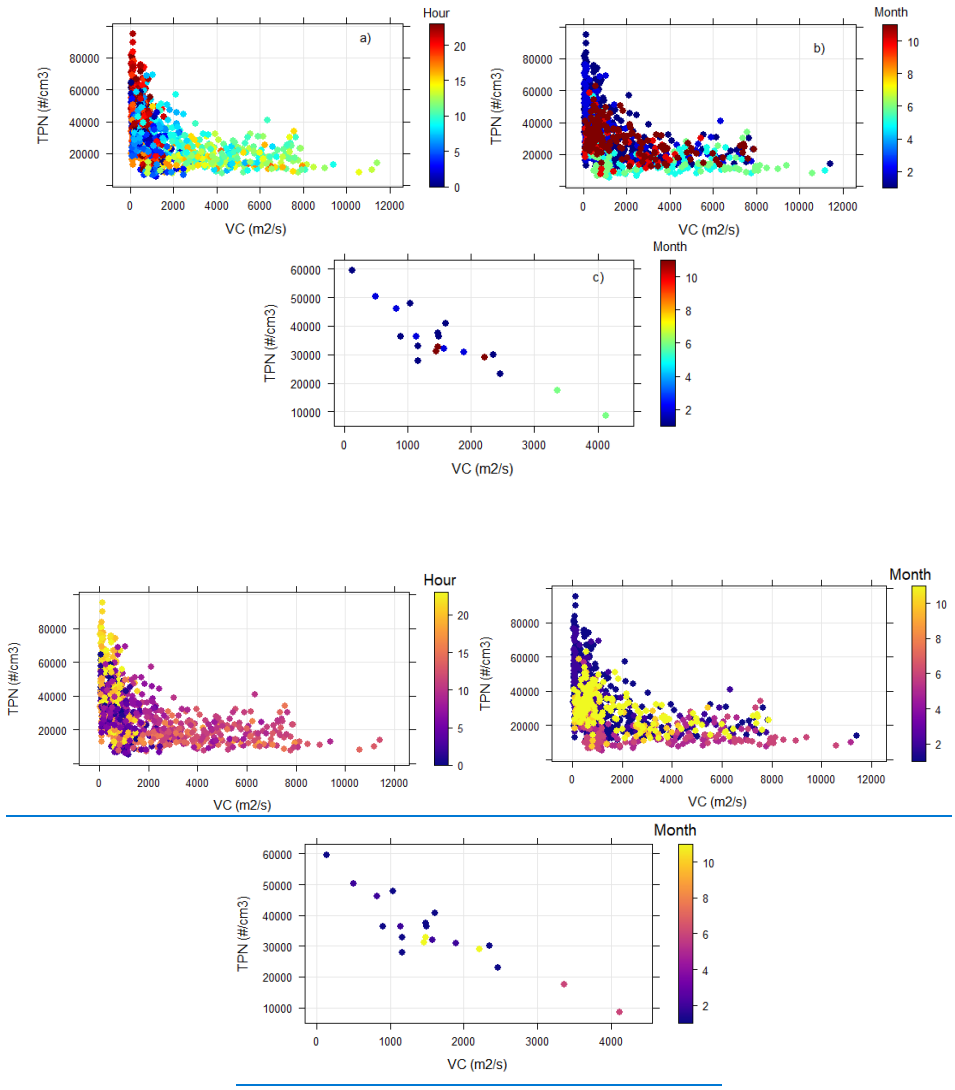

Figure S8: Variations of Total Particle Number (TPN) as a function of ventilation coefficient (VC). a) and b): Each scatter point is a hourly average and is colour coded by hour and month. c): Each scatter point is a daily average and is colour coded by month. Note that the summer data is not enough to assess.

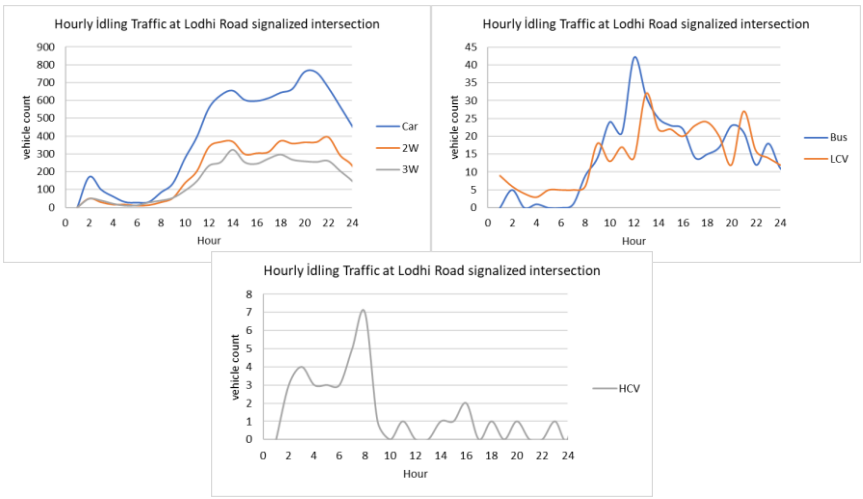

Figure S9: Hourly idling traffic at Lodhi Road signalized intersection in Delhi (data from Dhyani et al. 2019).

Table S3: Day and night summary of the wide range particle sizes derived from the merged data. Mean and standard deviation calculated by hourly data. The modes are based on SMPS and GRIMM observations. Nucleation = 10 - 25 nm, Aitken = 25-100 nm, Accumulation = 100-1000 nm, Large Fine = 1000-2500 nm, Coarse = 2500-10000 nm. UFP = Nucleation +Aitken, PN1 = UFP+Accumulation, PN10= PN1+Large Fine+Coarse, N/D = the ratio of Night to Day.

	Winter			Autumn			Summer		
	Day (N=252)	Night (N=284)	N/D	Day	Night	N/D	Day (105)	Night (111)	N/D
Number Concentration from GRIMM+SMPS									
Nucleation (#x10^3 cm^{-3})	1.3±0.5	1.6±0.5	1.3	1.2±0.5	1.3±0.7	1.1	0.8±0.4	0.8±0.2	1.0
Aitken (#x10^3 cm^{-3})	13.5±6.7	21.3±10.4	1.7	10.7±5.4	13.1±6.2	1.2	8.3±4.7	11.5±6.8	1.4
Accumulation (#x10^3 cm^{-3})	11.8±5.9	22.7±8.7	1.9	12.1±4.7	17.8±3.8	1.5	6.5 ±3.6	9.6±5.1	1.5
Large Fine (# cm^{-3})	10.1±8.6	13.0±7.6	1.3	6.1±5.8	8.5±7.3	1.4	7.7±5.9	13.1±11.3	1.7
Coarse (# cm^{-3})	1.6±1.3	1.8±1.2	1.1	1.1±0.6	1.1±0.6	0.9	1.9±0.9	2.2±1.2	1.2
UFP (#x10^3 cm^{-3})	14.7±7.6	22.9±11.3	1.6	13.0±6.5	15.1±7.7	1.1	9.1±5.5	12.3±7.0	1.3
PN1 (#x10^3 cm^{-3})	26.5± 13.5	45.6±20.0	1.7	25.0±11.1	33.3±12.5	1.3	15.6±9.1	21.9±12.1	1.4
PN10 (#x10^3 cm^{-3})	38.1±11.8	60.4±28.8	1.6	32.2±18.2	45.2±29.8	1.4	25.2±15.9	37.2±24.6	1.5
Mass Concentration									
Grimm+Smps-PM_1 (µg m^{-3})	202.7±103.3	340.3±109.3	1.7	259.5±151.8	357.7±182.8	1.4	84.8±47.5	121.8±62.3	1.4

Grimm+Smps $PM_{2.5}$ (µg m^{-3})	231.8±113.5	375.3±117.7	1.6	277.2±156.5	382.4±198.5	1.4	106.4±55.5	151.5±76.5	1.4
Grimm+Smps PM_{10} (µg m^{-3})	377.3±161.5	532.5±175.9	1.4	362.1±159.5	455.3±198.1	1.2	260.2±122.6	331.8±171.8	1.3
Teom-$PM_{2.5}$ (µg m^{-3})	158.0±78.9	196.3±84.0	1.2	214.8±121.3	228.5±112.5	1.0	117.2±53.8	123.7±56.2	1.0
BC (µg m^{-3})	5.0±4.0	14.8±11.7	2.9	11.4±7.8	20.1±9.0	1.8	11.2±9.5	5.2±3.5	2.1
NO (ppb)	17.6±42.4	103.9±99.8	6.1	32.9±58.5	123.8±85.8	3.7	4.4±12.7	107.1±127.8	26.5
NO2 (ppb)	59.5±28.0	76.7±25.5	1.3	88.2±44.0	69.5±21.0	0.8	40.3±34.0	87.2±49.4	2.1

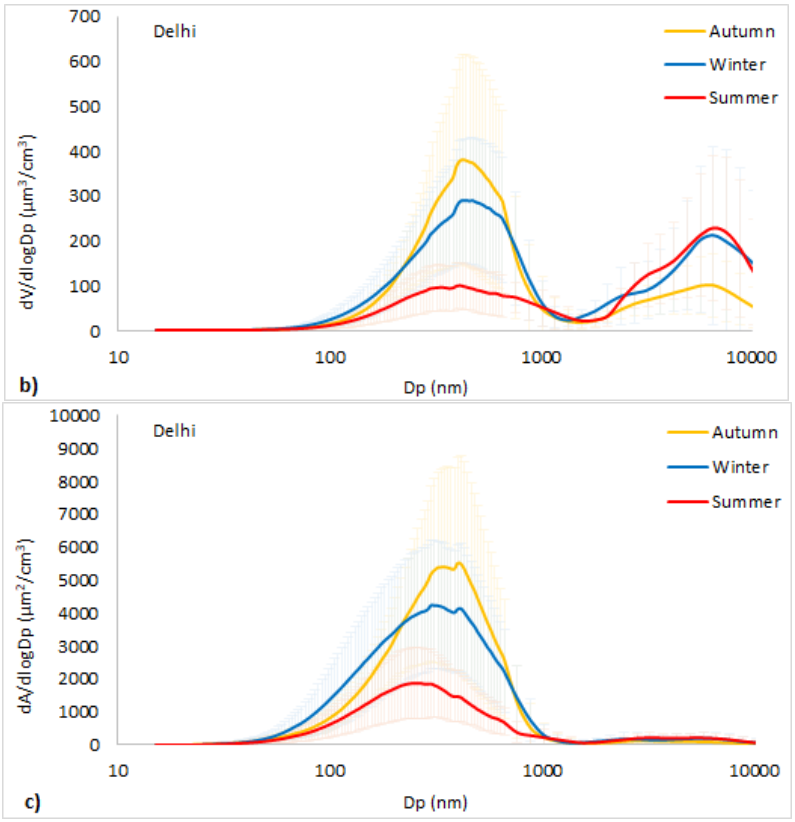

Figure S10: Hourly average particle number (a), volume (b) and area (c) distributions derived from the SMPS and Grimm instruments in autumn, summer and winter in Delhi. (Between 15 nm and 10000nm).

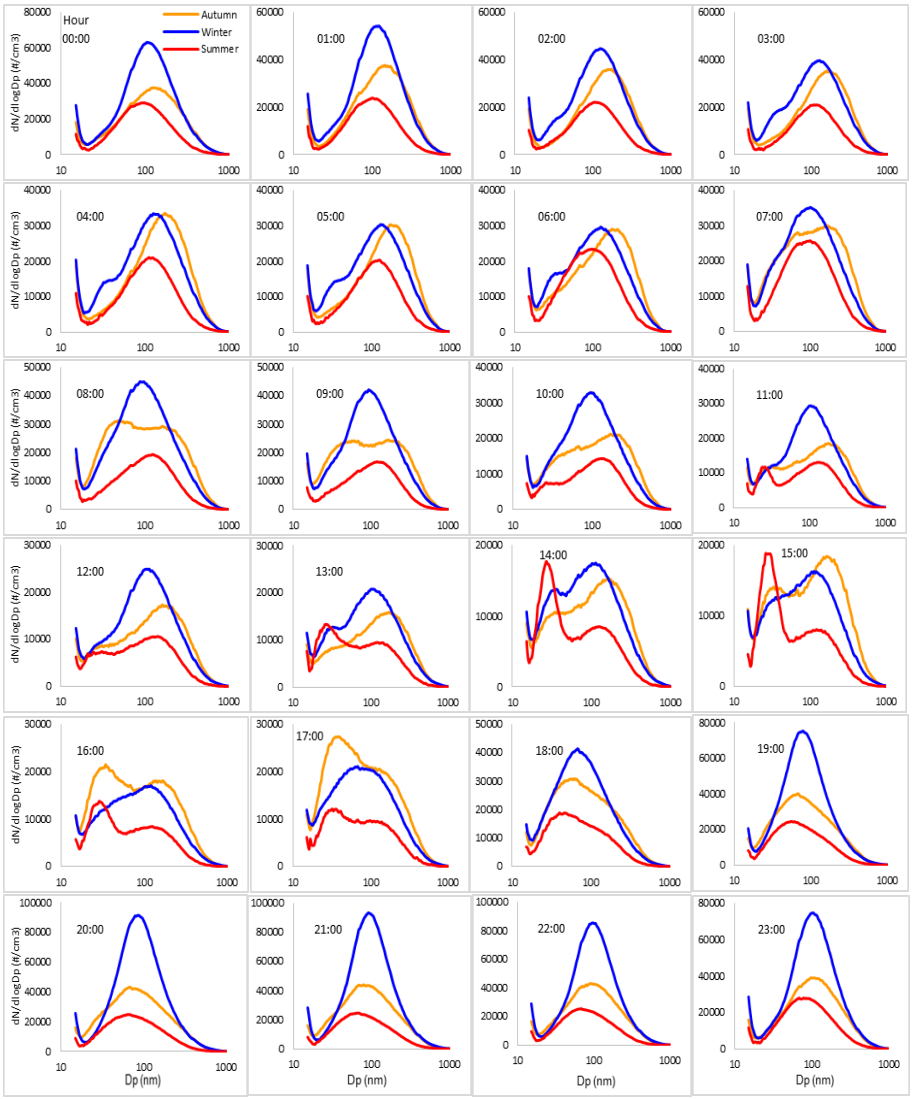

Figure S11: Average PSD for each hour and season in Delhi.

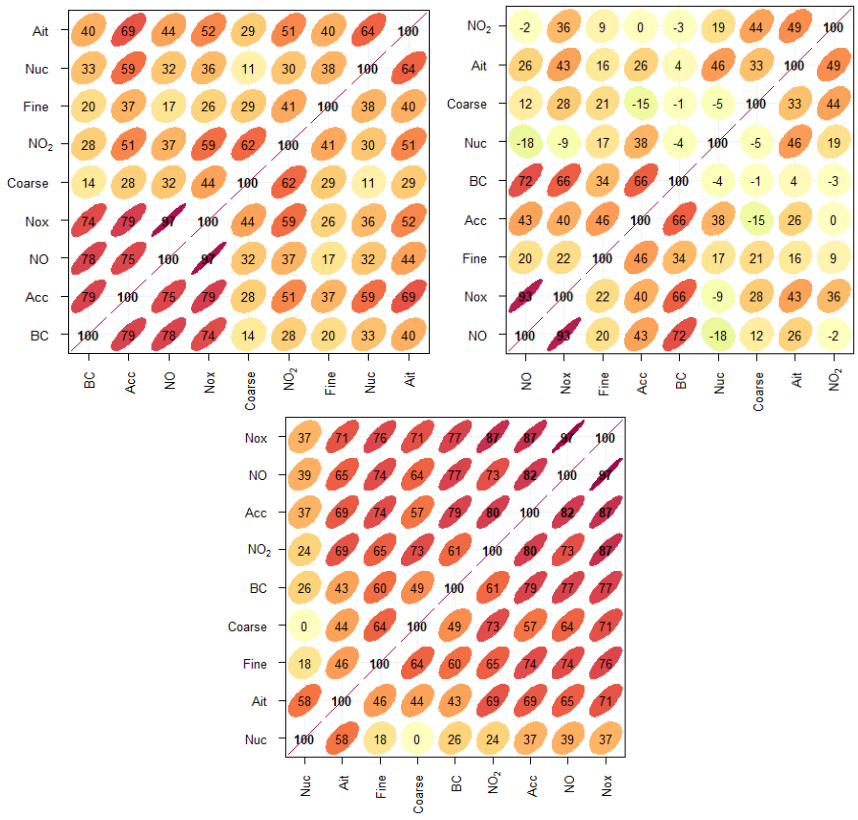

Figure S12: Correlation coefficients (x100) of PN within size fractions and NO, NO_2, BC.

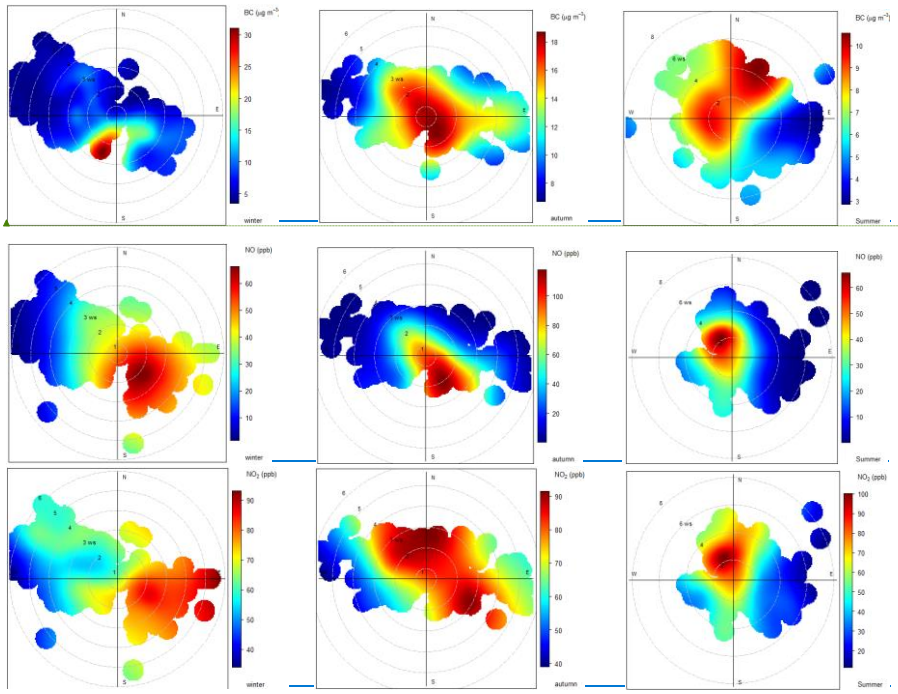

Formatted: Font: (Default) Times New Roman, 0 pt, Font color: Black, Character scale: 0%, Border: : (No border), Pattern: Clear (Black)

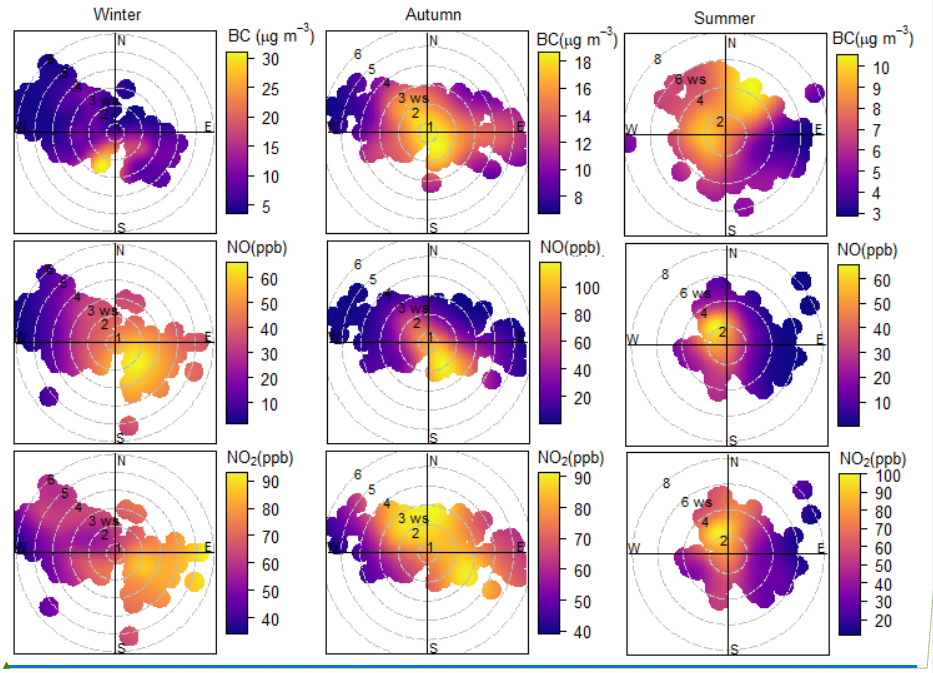

Figure S13: Polar plots of BC (top panels) NO, NO_2 (bottom panels) in winter (left), autumn (midle) and summer (right) in Delhi.

Formatted: Font: (Default) Times New Roman, 12 pt, Bold